

PAM: Plaid Atoms Model for Bayesian Nonparametric Analysis of Grouped Data

Dehua Bi¹ and Yuan Ji¹

¹Department of Public Health Sciences, The University of Chicago, IL

May 1, 2023

Abstract

We consider dependent clustering of observations in groups. The proposed model, called the plaid atoms model (PAM), estimates a set of clusters for each group and allows some clusters to be either shared with other groups or uniquely possessed by the group. PAM is based on an extension to the well-known stick-breaking process by adding zero as a possible value for the cluster weights, resulting in a zero-augmented beta (ZAB) distribution in the model. As a result, ZAB allows some cluster weights to be exactly zero in multiple groups, thereby enabling shared and unique atoms across groups. We explore theoretical properties of PAM and show its connection to known Bayesian nonparametric models. We propose an efficient slice sampler for posterior inference. Minor extensions of the proposed model for multivariate or count data are presented. Simulation studies and applications using real-world datasets illustrate the model's desirable performance.

Keywords: Clustering; Dependent clustering; Dirichlet process; MCMC; Slice sampler; Stick-breaking process.

1 Introduction

Clustering, or unsupervised learning, is a primary tool for data analysis and scientific exploration. Representative clustering methods include algorithmic approaches like K-Means [MacQueen, 1967] and model-based clustering like MClust [Fraley and Raftery, 1998]. Alternatively, Bayesian nonparametric (BNP) models like the Dirichlet process (DP) [Ferguson, 1973] induce clusters naturally through their property of allowing ties among observations. These ties are also referred to as atoms in some literature, e.g., in Denti et al. [2021]. Hereafter, we use “clusters” and “atoms” interchangeably.

For complex problems and data structures, dependent clustering is often necessary. For example, in linguistic research, it is of interest to discover common themes across multiple documents [Teh et al., 2004], where the themes are modeled as shared clusters. In biomedical research, modern experiments routinely generate high-throughput “-omics” data for multiple subjects. It is desirable to identify shared features across subjects, where a feature is often defined as a cluster of molecular units (e.g., genes). A common question for many dependent clustering problems is whether a clustering method can simultaneously cluster the observations within each group and capture the shared clusters across all or some groups. A group could be an individual subject or a scientific study, and observations could be genes of the subject or experimental units for the study. Various dependent clustering approaches have been proposed in the literature. For instance, Teh et al. [2004] pioneered a hierarchical DP (HDP) model to cluster observations arranged in groups. Through the use of a DP prior as the base measure for another DP model, the authors built a foundation for generating clusters that are common across the groups but with varying weights. In other words, all groups share the same atoms (clusters) but with different weights (sizes). Rodriguez et al. [2008] proposed a different structure called the Nested DP (NDP), which induces two layers of clusters, one for the groups and the other for the observations within

each group. As a result, observations within each group form observational clusters, and groups sharing the same observational clusters form distributional clusters. Groups belonging to the same distributional cluster have the same atoms and weights for the observational clusters, which is different from HDP. In other words, under NDP if two groups have the same atoms, they must also have the same weights. This is referred to a phenomenon called “degeneracy” [Camerlenghi et al., 2019]. Conversely, due to its construction it is impossible for HDP to produce identical weights for observational clusters across different groups. With probability one, the weights of atoms under HDP are different across groups.

Recognizing the properties of HDP and NDP, Camerlenghi et al. [2019] proposed a latent nested process (LNP) model based on common and group-specific completely random measures (CRMs). The LNP model allows groups to have common or unique clusters, and if common, identical weights. More recently, Denti et al. [2021] proposed a common atoms model (CAM) that allows common atoms with different or identical weights across groups, with more efficient computation. Table A.1 in Appendix A.1 summarizes the features of these BNP models, along with our proposed model, called the plaid atoms model (PAM). Other BNP models have been proposed to generate various dependent clustering structures, including the semi-HDP [Beraha et al., 2021] and hidden-HDP [Lijoi et al., 2022], which are not thoroughly reviewed due to space limits.

Our research is motivated by the need to generate novel dependent clustering structures across groups that allow for both common and unique atoms. We use the term “plaid atoms” to represent this structure, hence the name plaid atoms model (PAM). Under PAM, two groups may share a subset of common atoms but also possess unique ones. For example, two documents may both cover Roman history, but only one document includes the theme of religion. Similarly, two clinical trials may share subpopulations of adult patients with similar characteristics, but only one trial consists of pediatric patients. Therefore, in PAM, we generalize existing work by proposing plaid atoms that include both common and unique

ones across groups. The dependent clustering is governed by a hierarchical BNP model that uses a zero-augmented beta (ZAB) distribution in a stick-breaking representation [Sethuraman, 1994] of the HDP. This allows the weight of an atom to be exactly zero in some groups but not in others, thereby effectively removing the atom from some groups. Therefore, the atom possessed by the remaining groups is common and shared by these groups. A unique atom for a group can be generated when that atom is removed from all the other groups.

Along with PAM, we also propose a marginal process for data from a single group. The process, called the fractional stick-breaking process (FSBP), is the mean process of PAM and possesses interesting and useful properties that are connected to known BNP models. In the theoretical discussion, we derive results for both models, FSBP and PAM. However, in the application of this paper, we focus on PAM as it is the main motivation and interests of this work. We propose an efficient computational approach based on the slice sampler [Kalli et al., 2011], following the work in Denti et al. [2021], but with substantial modification to accommodate the ZAB construction. Inference under PAM provides useful estimates to describe the clustering results and accuracy in data analysis. Lastly, we implement PAM for datasets with either univariate or multivariate observations, allowing PAM to be applied in a wide range of applications.

The remaining sections of the article are as follows. In Section 2, we introduce the PAM for both continuous and count data, as well as the FSBP. Section 3 discusses the theoretical properties of FSBP and PAM. In Section 4, we discuss posterior inference and outline the slice sampler algorithm for PAM. Section 5 compares the performance of our proposed method with other models through simulation studies. Section 6 applies the proposed model to two publicly available datasets. Section 7 concludes the paper with some discussion.

2 Two Proposed Models

2.1 Overview

We will begin by presenting the proposed general model, PAM, for grouped data analysis, followed by a discussion of the fractional stick-breaking process (FSBP), which is the mean process of PAM. Consider a dataset with J groups of observations, where each group j consists of n_j observations of dimension $p \geq 1$. Denote the i th observation in j th group by $\mathbf{y}_{i,j} = (y_{i,j,1}, \dots, y_{i,j,p})$, $i = 1, \dots, n_j$, and let $\mathbf{y}_j = \{\mathbf{y}_{1,j}, \dots, \mathbf{y}_{n_j,j}\}$ represent all the observations in group j , $j = 1, \dots, J$. Assume that each observation $\mathbf{y}_{i,j}$, $i = 1, \dots, n_j$ and $j = 1, \dots, J$ takes a value from X , a suitable Polish space endowed with the respective Borel σ -field \mathcal{X} . Our goal is to partition observations \mathbf{y}_j within each group into clusters, allowing some but not all clusters to be shared with clusters in other groups.

2.2 Plaid Atoms Model – Continuous Data

Assume observation $\mathbf{y}_{i,j}$ (could be a scalar or vector) arises from a nonparametric mixture model indexed by parameter $\boldsymbol{\theta}_{i,j}$ and a random distribution G_j . Mathematically, we write

$$\mathbf{y}_{i,j} | \boldsymbol{\theta}_{i,j} \sim F(\mathbf{y}_{i,j} | \boldsymbol{\theta}_{i,j}), \quad \boldsymbol{\theta}_{i,j} | G_j \sim G_j, \quad i = 1, \dots, n_j; \quad j = 1, \dots, J,$$

where $F(\cdot | \boldsymbol{\theta}_{i,j})$ is a parametric distribution for $\mathbf{y}_{i,j}$. BNP models assume G_j follows a nonparametric prior distribution. For example, in HDP [Teh et al., 2004], each G_j is assigned a DP prior with base measure G_0 , which itself is an instance of DP , i.e.,

$$\begin{aligned} G_j | \alpha_0, G_0 &\sim \text{DP}(\alpha_0, G_0), \\ G_0 | \gamma, H &\sim \text{DP}(\gamma, H). \end{aligned}$$

Using the stick-breaking representation [Sethuraman, 1994] of DP, HDP can be rewritten as

$$\begin{aligned}
G_j &= \sum_{k=1}^{\infty} \pi_{j,k} \delta_{\phi_{\mathbf{k}}}, \pi_{j,k} = \pi'_{j,k} \prod_{l=1}^{k-1} (1 - \pi'_{j,l}) \\
\pi'_{j,k} &\sim \text{Beta} \left(\alpha_0 \beta_k, \alpha_0 \left(1 - \sum_{l=1}^k \beta_l \right) \right) \\
\phi_{\mathbf{k}} &\sim H, \text{ and } \quad \beta_k \sim \text{GEM}(\gamma)
\end{aligned} \tag{1}$$

where $\delta_{\{\cdot\}}$ is the indicator function, and GEM is the Griffiths-Engen-McCloskey distribution [Pitman, 2002]. Specifically, $\beta_k \sim \text{GEM}(\gamma)$ means that $\beta_k = \beta'_k \prod_{l=1}^{k-1} (1 - \beta'_l)$, and $\beta'_k \sim \text{Beta}(1, \gamma)$, where $\text{Beta}(a, b)$ denotes a beta distribution with mean $a/(a + b)$. Note that G_0 can be reconstructed from $\{\beta_k\}_{k=1}^{\infty}$ and $\{\phi_{\mathbf{k}}\}_{k=1}^{\infty}$ in equation (1) by $G_0 = \sum_{k=1}^{\infty} \beta_k \delta_{\phi_{\mathbf{k}}}$. Appropriate prior distributions like gamma can be specified for α_0 and γ to complete HDP. Since all G_j 's have the same set of atoms $\phi_{\mathbf{k}}$, by construction, the HDP model (1) assumes all groups share a set of common atoms. In the proposed PAM, we allow $\pi'_{j,k}$ to take the zero value for each group j , effectively removing atoms $\phi_{\mathbf{k}}$ from the group. Specifically, let $p_j \in (0, 1)$ denote a group-specific parameter that controls the proportions of atoms $\pi_{j,k}$'s to be retained (or removed with probability $1 - p_j$). Thus, we propose a zero-augmented beta (ZAB) for $\pi'_{j,k}$, given by,

$$f(\pi'_{j,k}) = p_j \times \underbrace{f_{\text{Beta}} \left(\alpha_0 \beta_k, \alpha_0 \left(1 - \sum_{l=1}^k \beta_l \right) \right)}_{(1)} + (1 - p_j) \times \underbrace{I(\pi'_{j,k} = 0)}_{\text{zero augmentation}}, \tag{2}$$

where $f_{\text{Beta}}(a, b)$ is the probability density function (p.d.f) of the beta distribution, and $I(A)$ is the indicator function for condition A . By replacing the beta prior distribution for $\pi'_{j,k}$ in (1) with (2), the proposed PAM as the prior distribution for G_j can be written as

follows:

$$\begin{aligned}
G_j &= \sum_{k=1}^{\infty} \pi_{j,k} \delta_{\phi_k}, \quad \pi_{j,k} = \pi'_{j,k} \prod_{l=1}^{k-1} (1 - \pi'_{j,l}) \\
f(\pi'_{j,k} | \boldsymbol{\beta}, p_j, \alpha_0) &= p_j \times f_{\text{Beta}} \left(\alpha_0 \beta_k, \alpha_0 \left(1 - \sum_{l=1}^k \beta_l \right) \right) + (1 - p_j) \times I(\pi'_{j,k} = 0) \\
\beta_k | \gamma &\sim \text{GEM}(\gamma), \quad \phi_k \sim H.
\end{aligned} \tag{3}$$

where $\boldsymbol{\beta} = \{\beta_k\}_{k=1}^{\infty}$. We use $G_j \sim \text{PAM}(\mathbf{p}, \alpha_0, \gamma, H)$ to denote (3), with $\mathbf{p} = \{p_1, \dots, p_J\}$. Priors need be placed on the parameters of \mathbf{p} , α_0 and γ , for example,

$$p_j | a, b \sim \text{Beta}(a, b), \alpha_0 \sim \text{Gamma}(a_\alpha, b_\alpha), \gamma \sim \text{Gamma}(a_\gamma, b_\gamma).$$

Adopting the parametrization in Denti et al. [2021] and Teh et al. [2004], and adding the sampling model for observation $\mathbf{y}_{i,j}$, the proposed PAM can be represented using a set of latent indicator variables $\mathbf{Z} = \{z_{i,j}\}_{\forall i,j}$ as cluster memberships for the observations. In other words, $z_{i,j} = k$ if observation i in group j is assigned to cluster k . Denoting $\boldsymbol{\pi}_j = \{\pi_{j,k}\}_{k=1}^{\infty}$, the proposed PAM mixture model is given by:

$$\begin{aligned}
\mathbf{y}_{i,j} | z_{i,j}, \phi_k &\sim F(\mathbf{y}_{i,j} | \phi_{z_{i,j}}), \\
z_{i,j} | \boldsymbol{\pi}_j &\sim \sum_{k=1}^{\infty} \pi_{j,k} \delta_k(z_{i,j}), \quad \pi_{j,k} = \pi'_{j,k} \prod_{l=1}^{k-1} (1 - \pi'_{j,l}), \\
f(\pi'_{j,k} | \boldsymbol{\beta}, p_j, \alpha_0) &= p_j \times f_{\text{Beta}} \left(\alpha_0 \beta_k, \alpha_0 \left(1 - \sum_{l=1}^k \beta_l \right) \right) + (1 - p_j) \times I(\pi'_{j,k} = 0).
\end{aligned} \tag{4}$$

The priors of $\boldsymbol{\beta}$ and ϕ_k remain the same as in (3), and the same priors can also be used for p_j , α_0 and γ . Except for the sampling distribution of $\mathbf{y}_{i,j}$ in (4), models (3) and (4) are equivalent. The notation G_j in (3) is replaced with $z_{i,j}$ in (4). This reparameterization is routinely used to facilitate posterior inference [Denti et al., 2021, Teh et al., 2004], which will be clear later on.

In equations (3) and (4), we use the Gaussian kernel for univariate observations $y_{i,j}$

($p = 1$) by setting $\phi_k = (\mu_k, \sigma_k^2)$ and $F(\cdot|\phi_k) = N(\cdot|\mu_k, \sigma_k^2)$. The base measure H is modeled as the conjugate prior of normal-inverse-gamma (NIG), where $H = \text{NIG}(\mu_0, \kappa_0, \alpha_0, \beta_0)$, i.e., $\mu_k|\sigma_k^2 \sim N(\mu_0, \sigma_k^2/\kappa_0)$ and $\sigma_k^2 \sim \text{IG}(\alpha_0, \beta_0)$. For multivariate observations ($p > 1$), $\phi_k = (\boldsymbol{\mu}_k, \boldsymbol{\Sigma}_k)$, where $\boldsymbol{\Sigma}_k$ is a $p \times p$ covariance matrix. We use $F(\cdot|\phi_k) = \text{MVN}(\cdot|\boldsymbol{\mu}_k, \boldsymbol{\Sigma}_k)$ to model multivariate Gaussian, and adopt the conjugate prior of normal-inverse-Wishart $H = \text{NIW}(\boldsymbol{\mu}_0, \nu_0, \kappa_0, \boldsymbol{\Psi})$, i.e., $\boldsymbol{\mu}_k \sim \text{MVN}(\boldsymbol{\mu}_0, \boldsymbol{\Sigma}_k/\nu_0)$ and $\boldsymbol{\Sigma}_k \sim \text{IW}(\boldsymbol{\Psi}, \kappa_0)$, where IW is the inverse-Wishart distribution.

2.3 Plaid Atoms Model – Count Data

Following Denti et al. [2021], we extend the proposed PAM to count data and refer to it as the Discrete Plaid Atoms Model (DPAM). Let the dimension of observation be $p = 1$. Let $x_{i,j} \in \mathbb{N}$ be the observed count data for observation $i = 1, \dots, n_j$ in group $j = 1, \dots, J$, where \mathbb{N} denotes the natural numbers. Thus the data vector $\mathbf{x}_j = (x_{1,j}, \dots, x_{n_j,j})$ is the set of counts observed for the j th group. We apply the data augmentation framework in Canale and Dunson [2011] and introduce latent continuous variables $y_{i,j}$ so that

$$\Pr(x_{i,j} = \omega) = \int_{a_\omega}^{a_{\omega+1}} g(y_{i,j}) dy_{i,j}, \quad \omega = 0, 1, 2, \dots \quad (5)$$

where $a_0 < a_1 < \dots < a_\infty$ is a fixed sequence of thresholds that take values $\{a_\omega\}_{\omega=0}^\infty = \{-\infty, 0, 1, 2, \dots, +\infty\}$, and $g(y_{i,j})$ follows the PAM mixture model as in equation (4). This construction allows posterior inference for $y_{i,j}$ since it is trivial to see that

$$x_{i,j}|y_{i,j} = \sum_{\omega=0}^{\infty} \mathbf{1}_\omega(x_{i,j}) \cdot \mathbf{1}_{[a_\omega, a_{\omega+1})}(y_{i,j}),$$

where $\mathbf{1}_a(b)$ equals 1 if $b = a$ or $b \in a$, and 0 otherwise.

2.4 Fractional Stick-breaking Process (FSBP)

We now introduce the new marginal process FSBP for data without grouping structure. This process is the mean of PAM. Let $\mathcal{P}(X)$ be the set of probability measures on (X, \mathcal{X}) . We define the fractional stick-breaking process (FSBP) as follows. Let $\bar{p} \in (0, 1]$ and $\gamma > 0$ be fixed constants. Furthermore, let H be a fixed, non-atomic distribution. For a random distribution $G^* \in \mathcal{P}(X)$, we denote $G^* \sim FSBP(\bar{p}, a, b, H)$ if for $k \geq 1$

$$\begin{aligned} G^* &= \sum_{k=1}^{\infty} \pi_k \delta_{\phi_k}, \quad \pi_k = \bar{p} \cdot \pi_k' \prod_{l=1}^{k-1} (1 - \bar{p} \cdot \pi_l'), \\ \pi_k' &\sim \text{Beta}(a, b), \quad \phi_k \sim H. \end{aligned} \tag{6}$$

Notice that we have slightly abused the notation by using π_k to denote the weight of G^* , which is similar to $\pi_{j,k}$ in equation (3). In section 3, we show that the mean process of the PAM model is the FSBP. Therefore, learning about FSBP sheds light on the theoretical properties of the more general but complex PAM model. Moreover, FSBP is also connected to many random probability measures (RPM) and stochastic processes in literature, which we briefly discuss next.

First of all, when $\bar{p} = a = 1$, FSBP becomes the usual stick-breaking process (SBP), hence the name FSBP. Since the stick-breaking process is equivalent to DP, we have $FSBP(1, 1, b, H) = DP(b, H)$. Second, when $\bar{p} < 1$, FSBP induces a different mechanism from SBP in generating the “breaks of sticks”. Instead of breaking π_k' portion of the stick for atom k in SBP, FSBP only breaks $\bar{p} \cdot \pi_k'$ portion. This means that each break is smaller but the remaining stick is longer. Third, FSBP is a special case of the kernel stick-breaking process (KSBP) of Dunson and Park [2008], where the kernel function is independent of the covariates and equal to a fixed constant of \bar{p} . The beta parameters are also fixed to a and b for all k , i.e., independent of the index k . Lastly, it is closely related to the geometric stick-breaking (GSB) RPM of Mena et al. [2011] if $\bar{p} = 1$, and we modify

equation (6) such that $\pi_k' = \pi'$ for all $k \geq 1$ and $\pi' \sim \text{Beta}(a, b)$.

3 Theoretical Properties of FSBP and PAM

3.1 Properties of FSBP

In this section, we explore the theoretical properties of the proposed FSBP and the PAM model. We first present results on FSBP. We assume $a = 1$ and $b = \gamma$ in FSBP so that it is closely related to the aforementioned BNP models. For simplicity, we denote $FSBP(\bar{p}, a = 1, b = \gamma, H)$ as $FSBP(\bar{p}, \gamma, H)$. In Theorem 1 below, we establish the mean and variance of $G^* \sim FSBP(\bar{p}, \gamma, H)$.

Theorem 1. *For an arbitrary set $A \subseteq X$, let $\bar{p} \in (0, 1]$ and $\gamma > 0$ be fixed constants, and H a fixed probability measure. For $G^* \sim FSBP(\bar{p}, \gamma, H)$, the mean and variance of G^* on A are*

$$E[G^*(A)] = H(A), \quad \text{Var}(G^*(A)) = \frac{H(A)\{1 - H(A)\}}{v}, \quad \text{where } v = \frac{1 + \gamma}{\bar{p}} + \frac{1 - \bar{p}}{\bar{p}}.$$

Remark 1. *The mean and variance of G^* match the mean and variance of a DP $G' \sim DP(v - 1, H)$.*

The proof of the theorem is in Appendix A.2. Theorem 1 shows that the mean and variance of FSBP and DP are connected.

We now derive the Exchangeable Partition Probability Function (EPPF) for G^* in a special case of FSBP, when $\gamma = 1$. The general case of $\gamma > 0$ has no closed-form results. The EPPF is the probability of a random partition of n samples from G^* , which is an almost surely discrete distribution. Specifically, according to its definition given by equation (6), G^* is an infinite mixture of point masses, denoted by $\Phi = \{\phi_1, \phi_2, \dots\}$. If we consider n

random samples from G^* , given by $\Theta = \{\theta_1, \dots, \theta_n\}$, where $\theta_i|G^* \sim G^*$ for $i = 1, \dots, n$, each θ_i takes a value in Φ with a probability. Therefore, ties might be generated among the θ 's. We assume Θ possesses K unique values taken from Φ , and denote these unique values by $\Phi_K = \{\phi_{r_1}, \dots, \phi_{r_K}\}$, where each r_k indexes the k th cluster and $r_k \in \mathbb{N} = \{1, 2, \dots\}$, the positive integers. Denote $\nabla = \{r_1, \dots, r_K\}$ the index set of the K clusters. Denote $\mathbf{z} = \{z_1, \dots, z_n\}$ the label vector where $\{z_i = k\}$ if θ_i is in cluster k , i.e., $\{\theta_i = \phi_{r_k}\}$. Let $c_k = \{i : z_i = k\}$ be the set of indices i 's for cluster k , i.e., $\forall i \in c_k, \theta_i = \phi_{r_k}$. Therefore, given \mathbf{z} , the set $C(\mathbf{z}) = \{c_k, r_k \in \nabla\}$ forms a partition of $\{1, \dots, n\}$. At last, the EPPF of G^* evaluated at a specific partition C of $\{1, \dots, n\}$ is defined as $\Pr(C(\mathbf{z}) = C)$ [Pitman, 1995]. Following the work of Miller [2019], we derive the expression of the EPPF of G^* when $\gamma = 1$ in the following theorem. For the upcoming discussion, notice that we denote S_K as the set of $K!$ permutations of $\{1, \dots, K\}$. That is, an element $\lambda \in S_K$ is a permutation of $\{1, \dots, K\}$, denoted as $\lambda = \{\lambda_1, \dots, \lambda_K\}$.

Theorem 2. *Let $\bar{p} \in (0, 1]$ be a fixed constant, and let H be a fixed probability measure. Let $G^* \sim \text{FSBP}(\bar{p}, 1, H)$. The EPPF of G^* for n samples is given by*

$$\frac{1}{\Gamma(n+1)} \left\{ \prod_{c \in C} \Gamma(|c|) \right\} \left\{ \prod_{c \in C} |c| \right\} \left[\sum_{\lambda \in S_K} \left\{ \prod_{k=1}^K (\xi_k \cdot (\alpha_k(\lambda) + 1) - 1)^{-1} \right\} \right],$$

where

$$\xi_k = \frac{\bar{p}}{F(\alpha_{k+1}(\lambda); \alpha_k(\lambda) + 1, 1 - \bar{p})},$$

$\Gamma(\cdot)$ is the gamma function, $|c|$ denotes the cardinality of the set c , $F(\cdot; n, p)$ is the CDF of a binomial distribution with size n and success probability p , $\alpha_k(\lambda) = |c_{\lambda_k}| + |c_{\lambda_{k+1}}| + \dots + |c_{\lambda_K}|$, and c_{λ_k} is the λ_k 's component of C . When $\bar{p} \rightarrow 1$, we have $\xi_k \rightarrow 1$, and the EPPF of G^*

converges to the EPPF of $G_0 \sim DP(1, H)$, which is given by

$$\frac{1}{\Gamma(n+1)} \left\{ \prod_{c \in C} \Gamma(|c|) \right\}.$$

The proof of theorem 2 is given in appendix A.3. Theorem 2 establishes the connection of FSBP and DP in its EPPFs.

We next explore the clustering property of the FSBP. Returning to the general case where $\gamma > 0$, we will show that the expected number of clusters in G^* is greater than the expected number of clusters in the corresponding DP with $G_0 \sim DP(\gamma, H)$. The first lemma shows the probability of forming a new cluster with the i th sample θ_i , i.e., $\theta_i \notin \{\theta_1, \dots, \theta_{i-1}\}$, when they are generated from FSBP.

Lemma 1. *Let $\bar{p} \in (0, 1]$ and $\gamma > 0$ be fixed constants, and let H be a fixed probability measure. Let $G^* \sim FSBP(\bar{p}, \gamma, H)$, and let $\theta_1, \dots, \theta_i | G^* \sim G^*$. Denote w_i as a binary indicator for the i th sample θ_i , such that*

$$w_i = \begin{cases} 1 & \text{if } \theta_i \notin \{\theta_1, \dots, \theta_{i-1}\} \\ 0 & \text{o.w.} \end{cases},$$

then, for $i \geq 2$,

$$Pr(w_i = 1 | \bar{p}, \gamma) = 1 - \sum_{k=2}^i (-1)^k \binom{i-1}{k-1} \frac{(k-1)!}{\prod_{l=1}^k (l+k)} \frac{(\gamma+1)\bar{p}^{k-1}}{{}_2F_1(1, 1-k; \gamma+2; \bar{p})}$$

where ${}_2F_1(a, b; c; z)$ is the hypergeometric function [Abramowitz et al., 1988].

The proof of Lemma 1 is in Appendix A.4. Next, we consider a special case of G^* , where $\bar{p} = 1$ (in this case, G^* reduces to $G_0 \sim DP(\gamma, H)$). In this case, the probability of forming

a new cluster with the i th sample θ_i coincides with that of the DP:

Lemma 2. *Let $\bar{p} = 1$ in Lemma 1, then*

$$Pr(w_i = 1 | \bar{p} = 1, \gamma) = \frac{\gamma}{\gamma + i - 1}.$$

The proof of Lemma 2 is in Appendix A.5. Notice that the result in Lemma 2 corresponds to the probability when the i th sample θ_i is drawn from the base measure H in a Polya urn scheme in DP [Ferguson, 1973]. Based on Lemma 1 and 2, we have the following theorem.

Theorem 3. *Let $\bar{p} \in (0, 1]$, $\gamma > 0$ be fixed constants, and w_i be defined as in Lemma 1. Then*

$$Pr(w_i = 1 | \bar{p}, \gamma) \geq \frac{\gamma}{\gamma + i - 1}.$$

The proof of Theorem 3 is shown in Appendix A.6. The following corollary follows directly from Theorem 3:

Corollary 1. *Let n^* be the prior number of clusters of $G^* \sim FSBP(\bar{p}, \gamma, H)$ on n samples. The prior expected number of clusters is*

$$E[n^* | \bar{p}, \gamma] = 1 + \sum_{i=2}^n Pr(w_i = 1 | \bar{p}, \gamma).$$

Let n_0 be the prior number of clusters of $G_0 \sim DP(\gamma, H)$ on n samples. The prior expected number of clusters in this case is

$$E[n_0 | \gamma] = \sum_{i=1}^n \frac{\gamma}{\gamma + i - 1}.$$

Additionally, we have

$$E[n^*|\bar{p}, \gamma] \geq E[n_0|\gamma] \approx \gamma \log \left(\frac{\gamma + n}{\gamma} \right).$$

Remark 2. *The FSBP has a higher prior expected number of clusters than DP.*

We also hypothesize that the prior expected number of clusters for FSBP decreases with \bar{p} , although the proof of this hypothesis is left for future work as it involves complicated maneuver of hypergeometric functions. Next, we derive properties related to PAM and show the FSBP is the mean process of PAM.

3.2 Properties of PAM

When $p_j = 1$ for all $j = 1, \dots, J$, equations (1) and (3) are identical. In other words, HDP is a special case of PAM when $p_j = 1$ for all j . Now, with $p_j \sim \text{Beta}(a, b)$, we show that PAM is a proper discrete distribution (Proposition 1) and observations belonging to two groups and generated from PAM have a positive probability to be equal, thereby forming clusters (Proposition 2).

Proposition 1. *Assume $G_j \sim \text{PAM}(\mathbf{p}, \alpha_0, \gamma, H)$ where PAM is defined in (3). Also, assume $p_j \sim \text{Beta}(a, b)$ for $j = 1, \dots, J$. Then*

1. $\sum_{k \geq 1} \pi_{j,k} = 1$, and
2. $E[\pi_{j,k}] = \frac{1}{1+\gamma'} \left(\frac{\gamma'}{1+\gamma'} \right)^{k-1}$ where $\gamma' = \frac{1+\gamma-\bar{p}}{\bar{p}}$, $\bar{p} = \frac{a}{a+b}$.

Note that we use \bar{p} to represent the prior mean of p_j . This will correspond to the parameter \bar{p} in FSBP as shown in Theorem 4.

Proposition 2. Let $G_1, \dots, G_J \sim \text{PAM}(\mathbf{p}, \alpha_0, \gamma, H)$. Without loss of generality, for two groups G_1 and G_2 , let $\boldsymbol{\theta}_{i,1}|G_1 \sim G_1$ and $\boldsymbol{\theta}_{i',2}|G_2 \sim G_2$, then

$$\Pr(\boldsymbol{\theta}_{i,1} = \boldsymbol{\theta}_{i',2}) > 0. \quad (7)$$

The proofs of Propositions 1 and 2 are in Appendix A.7 and A.8, respectively. The second proposition is trivial but necessary to verify PAM as a proper model choice for clustering on grouped data. Moreover, the first proposition is important in which not only it establishes the correctness of G_j as a discrete distribution, but it also leads to the derivation of the mean process of G_j in the next theorem.

Theorem 4. For an arbitrary set $A \subseteq X$, let $\alpha_0, \gamma > 0$, H be a fixed probability measure, $G_0 \sim \text{DP}(\gamma, H)$, and $G_j \sim \text{PAM}(\mathbf{p}, \alpha_0, \gamma, H)$ where PAM is defined in (3) and $\mathbf{p} = \{p_1, \dots, p_J\}$. Further assume $p_j \sim \text{Beta}(a, b)$ for $j = 1, \dots, J$. Then, the conditional mean of G_j is given by

$$E[G_j(A)|G_0] = G^*(A),$$

where $G^* \sim \text{FSBP}(\bar{p}, \gamma, H)$, $\bar{p} = a/(a + b)$.

The proof of Theorem 4 is given in Appendix A.9. This theorem shows that the mean process of PAM is FSBP. As a consequence of Theorem 1 of FSBP, the marginal mean of G_j follows directly and is shown in the following corollary:

Corollary 2. $E[G_j(A)] = E[E[G_j(A)|G_0]] = E[G^*(A)] = H(A)$.

Unfortunately, there are no closed-form results for the partition probability functions, including the EPPF with $J = 1$ and the partial exchangeable partition probability function (pEPPF) with $J > 1$ for PAM, and the expected number of clusters for PAM is not available

in closed-form either. However, since we have now shown the mean of PAM is FSBP, the EPPF and expected number of clusters for FSBP in the previous section provide a clue on the average behavior of PAM. Specifically, the mean process of PAM induces more clusters on average than DP.

4 Posterior Inference

4.1 Overview

Posterior inference under PAM utilizes a modified and efficient slice sampler proposed by Denti et al. [2021]. A simpler approach based on the Chinese Restaurant Franchise (CRF) process in Teh et al. [2004] that can be applied for the inference of HDP does not work for PAM, unfortunately, due to the group-specific zero weights in the proposed ZAB construction. An alternative inference method for PAM could be the truncated blocked-Gibbs sampler in Rodriguez et al. [2008], which approximates the infinite mixture in equation (3) with a finite mixture. However, such an approximation can introduce errors in the inference [Denti et al., 2021, Rodriguez et al., 2008]. The proposed slice sampler is illustrated for univariate observations (i.e., $p = 1$), and can be easily extended to accommodate multivariate observations (i.e., $p > 1$) or the DPAM model.

4.2 Slice Sampler

By integrating out $z_{i,j}$ in equation (4), we can rewrite the density function for $y_{i,j}$ as an infinite mixture as

$$f(y_{i,j}|\Phi, \pi_j) = \sum_{k \geq 1} \pi_{j,k} \cdot p(y_{i,j}|\phi_k), \quad (8)$$

where $\Phi = \{\phi_k\}_{k \geq 1}$. Following Kalli et al. [2011], we use a set of uniformly distributed random variables $\mathbf{u} = \{u_{i,j}\}$ to separate the “active” mixture components from the other

“inactive” components, which will become clear next. By definition, each $u_{i,j} \sim \text{Unif}(0, 1)$. Additionally, we consider J deterministic probabilities $\boldsymbol{\xi}_j = \{\xi_{j,k}\}_{k \geq 1}$ for a fixed j , where $\xi_{j,k} \equiv \xi_k = (1 - \zeta)\zeta^{k-1}$ and $\zeta \in (0, 1)$ is a fixed parameter with a default value of 0.5, and $\boldsymbol{\xi}_j \equiv \boldsymbol{\xi} = \{\xi_k\}_{k \geq 1}$. A more complicated construction may allow different ζ_j for different groups j , which we do not consider here. As a result, the augmented likelihood for observation $y_{i,j}$ can be expressed as:

$$f_{\boldsymbol{\xi}}(y_{i,j}, u_{i,j} | \boldsymbol{\Phi}, \boldsymbol{\pi}_j) = \sum_{k \geq 1} \mathbf{1}_{\{u_{i,j} < \xi_k\}} \frac{\pi_{j,k}}{\xi_k} p(y_{i,j} | \phi_k) \quad (9)$$

Integrating with respect to $u_{i,j}$ returns $f(y_{i,j} | \boldsymbol{\Phi}, \boldsymbol{\pi}_j)$ in (8). Now adding the cluster indicator $z_{i,j}$ in (4), we express (9) as

$$f_{\boldsymbol{\xi}}(y_{i,j}, u_{i,j} | z_{i,j}, \boldsymbol{\Phi}, \boldsymbol{\pi}_j) = \sum_{k \geq 1} \mathbf{1}_{\{z_{i,j} = k\}} \mathbf{1}_{\{u_{i,j} < \xi_{z_{i,j}}\}} \frac{\pi_{j,z_{i,j}}}{\xi_{z_{i,j}}} p(y_{i,j} | \phi_{z_{i,j}}). \quad (10)$$

The proposed slice sampler follows a Gibbs-sampler style, in which it iteratively samples the following parameters,

1. $u_{i,j} | \dots \propto I(0 < u_{i,j} < \xi_{z_{i,j}})$,
2. the stick-breaking weights β'_k , $\pi'_{j,k}$, and p_j ,
3. the indicator $z_{i,j}$ with $\Pr(z_{i,j} = k | \dots) \propto \mathbf{1}_{\{u_{i,j} < \xi_k\}} \frac{\pi_{j,k}}{\xi_k} p(y_{i,j} | \phi_k)$, and
4. the atom location parameter $\phi_k | \dots \propto \prod_{z_{i,j} = k} N(y_{i,j} | \phi_k) p_H(\phi_k)$.

In the last step, since $\phi_k \sim H$, $p_H(\phi_k)$ denotes the prior density of H . The entire sampler is presented in Algorithm 1 next. Below we first describe the details of sampling $\pi'_{j,k}$ in step 2 above. The details of the entire slice sampler are in Appendix A.10.

In each iteration of the slice sampler, due to the introduction of latent uniform variates $u_{i,j}$ and the truncation on ξ_k , the infinite summation in equation (9) can be reduced to a

finite sum through “stochastic truncation”. To see this, first notice that $\{\xi_k\}$ is a descending sequence, and therefore only finitely many ξ_k ’s can meet the condition $1_{\{u_{i,j} < \xi_k\}}$. In other words, given \mathbf{u} , there exists a $K' \geq 1$ such that when $k \geq K'$, $\min_{i,j}(\mathbf{u}) \geq \xi_k$. This means that up to K' of the ξ_k ’s will be larger than a $u_{i,j}$. Let $K^* = K' - 1$. Then, noticing that $\xi_{K'} = (1 - \zeta)\zeta^{K'-1}$, we can easily show that

$$K^* = \left\lfloor \frac{\log(\min(\mathbf{u})) - \log(1 - \zeta)}{\log(\zeta)} \right\rfloor. \quad (11)$$

Here, K^* is called the “stochastic truncation” in the slice sampler. Given K^* , sampling β'_k is straightforward but requires a Metropolis-Hastings (MH) step (See Appendix A.10 for details). To sample $\pi'_{j,k}$, again conditional on K^* , let $\mathbf{Z}_j = \{z_{i,j}\}_{i=1}^{n_j}$, $m_{j,k} = \sum_{i=1}^{n_j} 1(z_{i,j} = k)$, and refer to the stick-breaking representation. The full conditional distribution of $\pi'_{j,k}$ is given by

$$p(\pi'_{j,k} | \dots) = p(\pi'_{j,k} | \mathbf{Z}_j, \boldsymbol{\beta}, p_j, \alpha_0) \propto \left[\pi'_{j,k} m_{j,k} (1 - \pi'_{j,k})^{\sum_{s=k+1}^{K^*} m_{j,s}} \right] f(\pi'_{j,k})$$

where $f(\pi'_{j,k})$ is defined in equation (2). When $m_{j,k} > 0$, it means cluster k in group j is not empty, and therefore $\pi'_{j,k} \neq 0$ (otherwise, it would not be possible to have a non-empty cluster k in group j). Hence, the full conditional of $\pi'_{j,k}$ is

$$p(\pi'_{j,k} | \dots) = f_{\text{Beta}} \left(\alpha_0 \beta_k + m_{j,k}, \alpha_0 \left(1 - \sum_{l=1}^k \beta_l \right) + \sum_{s=k+1}^{K^*} m_{j,s} \right). \quad (12)$$

Recall $f_{\text{Beta}}(\cdot)$ denotes a beta distribution density. When $m_{j,k} = 0$, which could mean $\pi'_{j,k} = 0$ or $\pi'_{j,k} \neq 0$ but the atom is not sampled, we have

$$p(\pi'_{j,k} | \dots) \propto (1 - \pi'_{j,k})^{\sum_{s=k+1}^{K^*} m_{j,s}} f(\pi'_{j,k}).$$

This can be expressed as

$$p(\pi'_{j,k}|\dots) = p_j^* \times f_{\text{Beta}}\left(\alpha_0\beta_k, \alpha_0\left(1 - \sum_{l=1}^k \beta_l\right) + \sum_{s=k+1}^{K^*} m_{j,s}\right) + (1-p_j^*) \times I(\pi'_{j,k} = 0) \quad (13)$$

where

$$p_j^* = \frac{p_j}{p_j + (1-p_j) \times \frac{B(\alpha_0\beta_k, \alpha_0(1-\sum_{l=1}^k \beta_l))}{B(\alpha_0\beta_k, \alpha_0(1-\sum_{l=1}^k \beta_l) + \sum_{s=k+1}^{K^*} m_{j,s})}}$$

and $B(a, b)$ is the beta function.

Lastly, sampling p_j and the concentration parameters follow standard MCMC simulation [Escobar and West, 1995], details of which is provided in Appendix A.10.

Additional step for count data Finally, for DPAM an additional step is added to update the latent continuous variable. Denote $\text{TN}(\mu, \sigma^2; a, b)$ the truncated normal distribution with mean μ , variance σ^2 , and boundaries a and b , the full conditional distribution of $y_{i,j}$ is

$$y_{i,j}|\dots \sim \text{TN}(\mu_{z_{i,j}}, \sigma_{z_{i,j}}^2; a_{x_{i,j}}, a_{x_{i,j}+1}). \quad (14)$$

Computation Algorithm Algorithm 1 introduces the proposed slice sampler. For multivariate observations, step 9 of Algorithm 1 can be replaced with a conjugate NIW prior, and multivariate normal can be used for $p(y_{i,j}|\phi_k)$ in step 8. On the other hand, the extension to DPAM can be achieved by adding steps to sample the latent $y_{i,j}$ according to equation (14) after step 7, and modifying the likelihood $p(y_{i,j}|\phi_k)$ in step 8 with

$$p(x_{i,j}|\phi_k) = \Delta\Phi(a_{x_{i,j}}|\phi_k) = \Phi(a_{x_{i,j}+1}|\phi_k) - \Phi(a_{x_{i,j}}|\phi_k),$$

where $\Phi(\cdot)$ denotes the cumulative distribution function (c.d.f) of the Gaussian distribution.

Algorithm 1 Slice-Efficient Sampler for PAM

- 1: **for** $t = 1, \dots, T$ **do**
- 2: Sample each $u_{i,j}$ from $u_{i,j} \sim \text{Unif}(0, \xi_{z_{i,j}})$ and find K^* in (11).
- 3: Sample all β'_k for $k = 1, \dots, K^*$ with MH step.
- 4: **for** each $\pi'_{j,k}$ for $j = 1, \dots, J$ and $k = 1, \dots, K^*$ **do**
- 5: **if** $m_{j,k} > 0$, sample $\pi'_{j,k}$ from (12). **otherwise**, sample $\pi'_{j,k}$ from (13).
- 6: **end for**
- 7: Sample $\mathbf{p} = \{p_j\}_{\forall j}$: denote $m_{j,0} = \sum_{k=1}^{K^*} 1(\pi'_{j,k} = 0)$,

$$p_j | \dots \sim \text{Beta}(a + K^* - m_{j,0}, b + m_{j,0})$$

- 8: Sample $\mathbf{Z} = \{z_{i,j}\}_{\forall i,j}$ from the following full condition:

$$p(z_{i,j} = k | \dots) \propto 1_{\{u_{i,j} < \xi_k\}} \frac{\pi_{j,k}}{\xi_k} p(y_{i,j} | \phi_k)$$

- 9: Sample ϕ_k from a conjugate NIG.
 - 10: **end for**
-

Label Switching As PAM involves an infinite mixture model, the issue of label switching can arise in MCMC samples [Papastamoulis, 2015]. To address the problem of label switching, we use the Equivalence Classes Representatives (ECR) algorithm described in Papastamoulis and Iliopoulos [2010]. Details of label-switching with the ECR method are in Appendix A.10.

4.3 Inference on Clusters

Like all BNP models, PAM produces random clusters and their associated posterior distributions. For a specific application, it is often desirable to report the common and unique clusters across groups. We discuss the corresponding inference under PAM next. We consider two approaches.

The first approach is through the MCMC samples of the label matrix $\mathbf{Z}^{(m)} = \{z_{i,j}^{(m)}\}$. For the m th MCMC iteration, vector $\mathbf{z}_j^{(m)} = \{z_{1,j}^{(m)}, \dots, z_{n,j}^{(m)}\}$ induces $k_j^{(m)}$ clusters. Let

$\mathbf{t}_j^{(m)} = \{t_1^{(m)}, \dots, t_{k_j}^{(m)}\}$ denote the labels of these clusters, which are the unique values of $\mathbf{z}_j^{(m)}$. Then the set and number of common clusters between groups j and j' are given by $\mathbf{t}_j \cap \mathbf{t}_{j'}$ and its cardinality, respectively, and the set and number of unique clusters for group j are given by $\mathbf{t}_j \text{ mod } \mathbf{Z} \setminus \mathbf{z}_j$ and its cardinality, respectively. Here, operation $A \text{ mod } B$ for two sets A and B is redefined as the unique elements in A but not B , and $\mathbf{Z} \setminus \mathbf{z}_j$ means the set after removing \mathbf{z}_j from \mathbf{Z} .

The second approach to summarize common and unique clusters is to use the posterior sample of the group-specific weights $\boldsymbol{\pi}_j^{(m)}$, $j = 1, \dots, J$. Specifically,

$$\begin{aligned}
 n_{\text{comm}}(\{\boldsymbol{\pi}_j^{(m)}, \boldsymbol{\pi}_{j'}^{(m)}\}) &= \sum_{k=1}^{|\boldsymbol{\pi}_j^{(m)}|} 1(\pi_{j,k}^{(m)} \neq 0 \text{ and } \pi_{j',k}^{(m)} \neq 0), \\
 n_{\text{uniq}}(\boldsymbol{\pi}_j^{(m)}) &= \sum_{k=1}^{|\boldsymbol{\pi}_j^{(m)}|} 1 \left(\pi_{j,k}^{(m)} \neq 0 \text{ and } \sum_{j'=\{1, \dots, j-1, j+1, \dots, J\}} \pi_{j',k}^{(m)} = 0 \right)
 \end{aligned} \tag{15}$$

where $|\cdot|$ denotes the cardinality of the corresponding vector. Thus, the weight approach is able to learn the same information as the \mathbf{Z} matrix method.

The above two approaches generate the same values of n_{comm} and n_{uniq} for each MCMC sample.

To produce a point estimate of the clustering result, we follow the approach in Wade and Ghahramani [2018] to estimate an optimal partition through a decision-theoretic approach that minimizes the variation of information [Meilă, 2007]. This optimal partition is then used as a "point estimate" of the random clusters obtained from PAM posterior inference.

5 Simulation Study

5.1 Simulation Setup

We test the performance of PAM through simulated univariate and multivariate data. We generate univariate observations based on scenario one in Denti et al. [2021], which assumes a finite mixture of Gaussian distributions. The second scenario assumes three groups of multivariate observations, with $p = 3$ and $J = 3$, where there is a combination of common and unique clusters among the groups.

Scenario 1 - Univariate data: Consider $J = 6$ groups. For group j , the observation follows a mixture of normal distributions

$$f(y_{i,j}) \propto \sum_{g=1}^j \frac{1}{g} N(m_g, \sigma^2), \quad i = 1, \dots, n_j,$$

where $m_g \in \{0, 5, 10, 13, 16, 20\}$, $\sigma^2 = 0.6$, and $j = 1, \dots, 6$. Therefore, there are j true clusters in group j defined by the j normals in $f(y_{i,j})$, with only the first cluster $N(m_1, \sigma^2)$ shared across all six groups. We test two sub-cases by setting the number of observations in group $n_j = n_A$, where $n_A \in \{50, 100, 150\}$, or by setting $n_j = n_B \times j$, where $n_B \in \{10, 20, 40\}$.

Scenario 2 - Multivariate data: This scenario assumes $p = 3$, $J = 3$ groups, and a total of five clusters. Observations are generated from a mixture of multivariate Gaussian distributions, with the mean and cluster weights shown in Table A.2 in Appendix A.11. Group 1 possesses all the clusters, group 2 has clusters 1, 3 and 4, and group 3 has clusters 2 and 3. The true covariance matrix is assumed to be the identity matrix, and we assume all groups have the same sample size, with $n_j = n$, where $n \in \{50, 100, 200\}$.

For the purpose of benchmarking, we compare the performance of the proposed PAM model with HDP and CAM. We assess the models' performance based on three criteria: 1)

the number of predicted clusters using the estimated optimal partition, with a value closer to the ground truth indicating better estimation, 2) the adjusted Rand index (ARI) [Hubert and Arabie, 1985] between the estimated optimal partition and the ground truth, with a value closer to 1 indicating better performance, and 3) the normalized Frobenius distance (NFD) [Horn and Johnson, 1990] between the estimated posterior pairwise co-clustering matrices and the true co-clustering structure, with a value closer to 0 indicating better performance. These metrics have been routinely adopted in the literature, e.g., in Denti et al. [2021].

5.2 Simulation Results

We adopt standard prior settings for the hyperparameters in Equation (3). Specifically, we use the NIG distribution as the base measure H , with hyperparameters $\mu_0 = 0$, $\kappa_0 = 0.1$, $\alpha_0 = 3$ and $\beta_0 = 1$. We use Jeffrey’s prior for p_j ’s, i.e., $a = b = 0.5$. Lastly, we set $a_{\alpha_0} = b_{\alpha_0} = a_{\gamma} = b_{\gamma} = 3$ for the gamma priors of the concentration parameters α_0 and γ . We collect an MCMC sample of 10,000 iterations after 10,000 iterations of burn-in. The Markov chains mix well.

Scenario One We generate 30 datasets for each sample size in sub-cases one and two, and apply three clustering methods, including the proposed PAM, as well as CAM and HDP, to these simulated data. We evaluate the performance of these methods based on three metrics: the total number of clusters, the ARI, and the NFD. The mean and standard deviation of each metric are reported in Table 1. The results demonstrate that PAM performs competitively with the other methods, especially when the sample size increases.

We also evaluate PAM’s ability to identify common and unique clusters across groups. To do so, we randomly select one simulated dataset with a group sample size 150 and present the data distribution for each group in Appendix A.11. We use group 6 as a reference since

Metrics	Methods	$n_A = 50$	$n_A = 100$	$n_A = 150$	$n_B = 10$	$n_B = 20$	$n_B = 40$
Number of clusters	CAM	4.03 (0.49)	4.67 (0.61)	4.97 (0.49)	4.17 (0.75)	4.40 (0.56)	5.43 (0.50)
	HDP	3.93 (0.53)	4.00 (0.59)	4.27 (0.58)	4.23 (0.50)	4.30 (0.65)	4.33 (0.61)
	PAM	4.93 (0.87)	5.67 (0.71)	5.97 (0.62)	5.77 (0.82)	6.00 (0.59)	6.17 (0.38)
ARI	CAM	0.90 (0.05)	0.93 (0.04)	0.95 (0.02)	0.79 (0.08)	0.83 (0.08)	0.93 (0.05)
	HDP	0.87 (0.05)	0.87 (0.05)	0.90 (0.04)	0.76 (0.08)	0.78 (0.09)	0.82 (0.07)
	PAM	0.87 (0.07)	0.91 (0.04)	0.95 (0.03)	0.73 (0.06)	0.82 (0.06)	0.94 (0.05)
NFD	CAM	0.07 (0.03)	0.07 (0.02)	0.07 (0.02)	0.08 (0.02)	0.08 (0.02)	0.05 (0.02)
	HDP	0.04 (0.02)	0.04 (0.02)	0.03 (0.01)	0.07 (0.03)	0.06 (0.03)	0.05 (0.02)
	PAM	0.06 (0.02)	0.04 (0.02)	0.02 (0.01)	0.09 (0.02)	0.06 (0.02)	0.02 (0.01)

Table 1: Simulated univariate data. Clustering performance for CAM, HDP, and PAM evaluated according to the number of total detected clusters (truth = 6 clusters) based on the estimated optimal clustering, the Adjusted Rand Index (ARI), and the normalized Frobenius distance (NFD). The entries are Mean (SD) over 30 datasets.

it contains all six clusters and investigate the number of common clusters between group 6 and the other groups, as well as the number of common clusters across all groups. Table A.3 in Appendix A.11 shows the results, and it appears that PAM is capable of capturing the unique cluster in group 6. Overall, all models perform similarly on this dataset.

Figure A.2 in Appendix A.11 reports the posterior distributions of the number of clusters in each group, the number of common clusters for group 6, and the number of unique clusters, according to the inference described in Section 4.3. The red vertical lines indicate the ground truth. Overall, the results look reasonable, especially on the common and unique clusters.

Scenario Two For the multivariate data, we use the following prior settings for the hyperparameters in (3). The NIW distribution is used as the base measure H , with hyperparameters $\boldsymbol{\mu}_0 = \mathbf{0} = \{0, 0, 0\}$, $\kappa_0 = 0.1$, $\nu_0 = 4$ and $\boldsymbol{\Psi} = I_3$, where I_3 is the 3×3 identity matrix. Similar to the univariate data, we use Jeffrey’s prior for p_j . We also set $a_{\alpha_0} = b_{\alpha_0} = a_\gamma = b_\gamma = 3$ in the gamma priors for the concentration parameters α_0 and γ . For simplicity, we only report the model accuracy on the number of clusters, ARI, and

NFD for this simulation. We generate 30 datasets for each sample size, and we summarize the results in Table 2.

Metrics	Methods	$n = 50$	$n = 100$	$n = 200$
Number clusters	CAM	5.40 (1.13)	5.37 (0.71)	5.04 (0.19)
	HDP	5.50 (0.97)	4.90 (0.76)	4.93 (0.47)
	PAM	4.93 (0.64)	5.07 (0.26)	5.03 (0.18)
ARI	CAM	0.90 (0.06)	0.95 (0.04)	0.97 (0.01)
	HDP	0.86 (0.11)	0.91 (0.07)	0.96 (0.02)
	PAM	0.89 (0.08)	0.96 (0.02)	0.97 (0.01)
NFD	CAM	0.05 (0.03)	0.04 (0.02)	0.03 (0.02)
	HDP	0.05 (0.02)	0.04 (0.02)	0.01 (0.01)
	PAM	0.03 (0.03)	0.01 (0.01)	0.01 (0.00)

Table 2: Simulated multivariate data. Clustering performance for CAM, HDP, and PAM evaluated according to the number of total detected clusters (truth = 5 clusters) based on the estimated optimal clustering, the Adjusted Rand Index (ARI), and the normalized Frobenius distance (NFD). The entries are Mean (SD) over 30 datasets.

The results indicate that all three methods have high accuracy in the multivariate data simulation. PAM performs competitively with the other two methods in terms of the ARI and NFD metrics when the sample size is large ($n \geq 100$).

6 Case Studies

In this section, we apply the proposed PAM method to two real-life datasets: a Microbiome dataset that studies the microbial distributions in African Americans and rural Africans [O’Keefe et al., 2015], and a Warts dataset of treating patients with warts using immunotherapy or cryotherapy. The former example demonstrates the use of the DPAM model for count data, while the latter shows the application of PAM to multivariate observations.

6.1 Microbiome Dataset

We begin by applying the DPAM model to the microbiome dataset, which was also analyzed by Denti et al. [2021]. This dataset, reported by O’Keefe et al. [2015], contains information on microbiota abundance for 38 healthy middle-aged African Americans (AA) and rural Africans (AF). The study aimed to investigate the effect of diet swap between individuals of AF and AA, as traditional foods for these populations differ. The 38 study participants were instructed to follow their characteristic diet, such as a low-fat and high-fiber diet for AF and a high-fat and low-fiber diet for AA, for two weeks, and then swap diets for another two weeks. We focus on the data obtained before the diet swap, and cluster subjects’ counts of operational taxonomic units (OTUs), which refer to clustered phylotypes based on taxonomical classification of microbial species obtained at the beginning of the experiment. The reported data are in the form of OTU counts (i.e., OTU expression) that record the numbers of recurrences of the corresponding OTUs in a particular ecosystem [Jovel et al., 2016, Kaul et al., 2017]. For more background, refer to O’Keefe et al. [2015] and Section 4 of Denti et al. [2021]. Hereafter, we use the term ”expression” and ”counts” interchangeably in this application.

In this dataset, each individual (AA or AF) is treated as a group, and the OTU counts are treated as subjects in each group. Following the same data-preprocessing steps as in Denti et al. [2021], we obtain 38 subjects (17 AF and 21 AA) with 119 OTUs. Note that all the OTUs are the same, so technically each group will never possess unique clusters of OTUs. In this application, by unique clusters, we mean unique expression of OTUs. In other words, we are clustering the counts of the OTUs, not the OTUs themselves. For illustrative purpose, we randomly select four subjects (i.e., four groups), two AAs (with IDs 5 and 22) and two AFs (with IDs 13 and 14). We remove the OTUs that had zero expression in all four individuals from the selected data. In the end, we obtain a dataset with $J = 4$ individuals (groups) and $n_j = 109$ OTUs (observations). The histograms of the

microbiome populations of the four selected individuals are shown in Appendix A.12.

For inference, similar to Denti et al. [2021], we incorporate the average OTU frequencies for subject j , denoted as $\eta_j = \frac{1}{n} \sum_{i=1}^n x_{i,j}$, as a scaling factor in the latent variable $y_{i,j}$ of the DPAM model. This leads to the following distribution:

$$y_{i,j} | \mathbf{Z}, \boldsymbol{\mu}, \boldsymbol{\sigma}^2 \sim N(\eta_j \mu_{z_{i,j}}, \eta_j^2 \sigma_{z_{i,j}}^2) \leftrightarrow \frac{y_{i,j}}{\eta_j} | \mathbf{Z}, \boldsymbol{\mu}, \boldsymbol{\sigma}^2 \sim N(\mu_{z_{i,j}}, \sigma_{z_{i,j}}^2) \quad (16)$$

The prior hyperparameters follow the same settings as in scenario one of simulation study, and we present the results with the optimal partition in Table 3.

PAM reports a total of eight estimated clusters across the four individuals: Clusters 1 and 2 are shared by all four individuals, cluster 7 is shared among individuals 5 (AF), 13 (AA), and 14 (AA), and cluster 8 is shared among individuals 5 and 22 (both from AF). The other clusters are unique to a specific individual. Based on the optimal partition of OTUs, we plot the taxa counts (TC) of OTUs grouped by all eight estimated clusters as well as by both clusters and individuals in Figure 1. Note that for easy demonstration of clusters across individuals, we have manually reordered the clusters in ascending order based on the cluster mean.

	Cluster 1	Cluster 2	Cluster 3	Cluster 4	Cluster 5	Cluster 6	Cluster 7	Cluster 8
Location	0.07(0.01)	0.53(0.04)	1.75(0.20)	1.50(0.26)	2.21(0.27)	3.73(0.36)	9.89(1.21)	74.21(8.99)
Weights	ID 5	0.56	0.26	0.11	0.00	0.00	0.00	0.05
	ID 22	0.84	0.12	0.00	0.00	0.00	0.02	0.00
	ID 13	0.77	0.11	0.00	0.00	0.10	0.00	0.02
	ID 14	0.74	0.10	0.00	0.11	0.00	0.00	0.05

Table 3: Posterior means of the atom locations $\boldsymbol{\mu}$ and weights $\boldsymbol{\sigma}$. Each entry in "Location" row represents posterior mean of $\mu(\sigma)$. Notice that the mean and SD are not scaled by η_j .

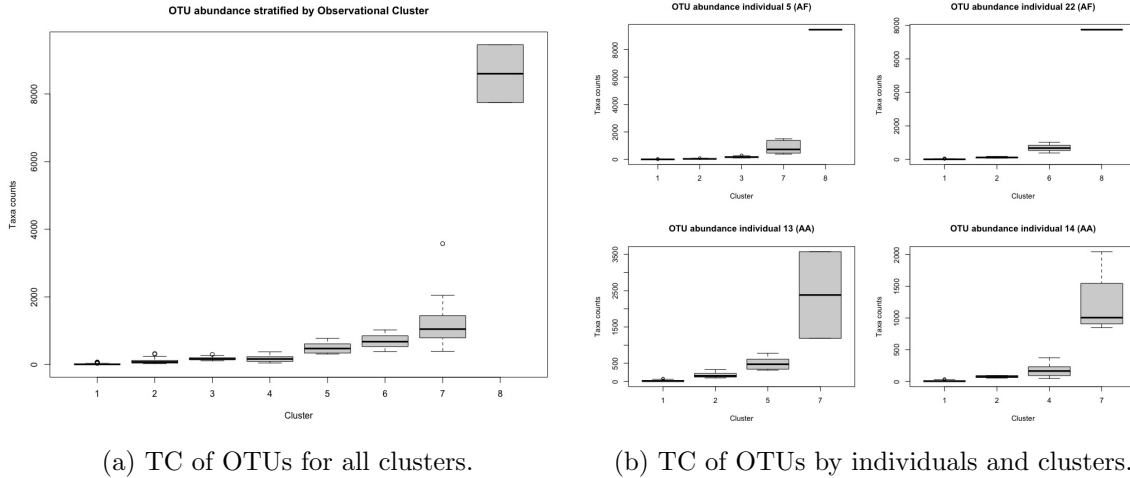


Figure 1: Boxplots of microbiome abundance counts stratified by clusters (a) and by both clusters and individuals (b).

We report an interesting finding related to the PAM clustering of OTUs. Specifically, OTU *Prevotella melaninogenica* is in cluster 8, which has the highest expression and is shared (both the cluster and the OTU) only by AF individuals 5 and 22. This finding is consistent with previous studies that have shown that the individuals with a predominance of *Prevotella spp.* are more likely to consume fiber, which is a typical component of an African diet [Graf et al., 2015, Preda et al., 2019].

We also applied DPAM to all 38 individuals and present the number of common clusters between each pair of individuals in a heatmap format in Figure A.4 in Appendix A.12. The heatmap uses a red color to indicate a higher number of common clusters shared by both individuals, while a white color indicates fewer common clusters. The results suggest that the individuals can be roughly divided into two clusters based on the heatmap, with individual 30 serving as the separating point. The cluster on the bottom left of the heatmap consists of 13 individuals from AF, with eight individuals from AA, while the top right cluster has 13 AAs and four AFs. In other words, one cluster is mostly composed of AFs,

while the other is dominated by AAs. A hierarchical clustering of the heatmap confirms the division of the individuals into two distinct groups.

6.2 Warts Dataset

In this example, we consider a publicly available dataset on warts which includes patients treated with two different options: immunotherapy and cryotherapy. Each treatment group contains medical records for 90 patients, and for each patient, six baseline characteristics (covariates) are reported, including the patient’s gender, age (Age), time elapsed before treatment (Time), the number of warts (NW), the type of warts (1-common, 2-plantar, 3-both), and the surface area of warts in mm^2 (Area). Additionally, patients’ responses to the corresponding treatments are also recorded.

To better understand potential differences between responders to the two treatments, we use PAM to cluster the covariate values of the responders. We use each treatment group as a separate group in PAM, with 71 responders in the immunotherapy group and 48 in the cryotherapy group. Therefore, $J = 2$. We exclude the binary covariate “gender” and the multinomial covariate “type of warts” from the analysis. Additionally, we treat the number of warts as a continuous variable. As a result, the final data set includes four covariates: Age, Time, NW, and Area. We set the hyperparameters of the priors to follow the same settings as in scenario two of the simulation, and the results are summarized below.

PAM identifies a total of seven clusters based on the optimal estimated clustering. Three of these clusters are common between the immunotherapy and cryotherapy groups, while the other four clusters are unique to either group. We summarize the posterior means of the four covariates and the weights for each of the seven clusters in Table 4. The table reveals that, among all responders, individuals with younger age, a short time elapsed from treatment (less than five months), and small surface area of warts form unique clusters in the cryotherapy group. On the other hand, those who were not treated for a longer

		Common			Unique in Immunotherapy		Unique in Cryotherapy	
		Cluster 1	Cluster 2	Cluster 3	Cluster 4	Cluster 5	Cluster 6	Cluster 7
Mean	Age	18.53	31.66	23.68	27.36	19.64	24.51	16.55
	Time	6.19	6.71	8.63	6.96	7.38	4.41	3.80
	NW	2.44	7.13	8.44	2.75	7.98	7.54	4.28
	Area	68.41	40.82	195.16	389.20	312.65	87.78	6.41
Weight	Immunotherapy	0.15	0.68	0.02	0.12	0.03	0.00	0.00
	Cryotherapy	0.31	0.17	0.06	0.00	0.00	0.36	0.10

Table 4: Posterior means of atom locations and atom weights for the inferred seven clusters. “Age” refers to the patient’s age, “Time” refers to time elapsed before treatment, “NW” refers to number of warts, and “Area” refers to the surface area of warts of the patient.

time and had a large surface area of warts (over 300 mm²) form distinct clusters in the immunotherapy group. Furthermore, it seems that the number of warts does not provide much information in determining a better treatment option for warts patients.

These findings are consistent with results from previously published studies. For instance, Khozeimeh et al. [2017b] found that patients younger than 24 years old showed a better response to cryotherapy, and patients who received cryotherapy within six months had a very high probability of being cured. This is consistent with the information implied by clusters 6 and 7, which are unique to the cryotherapy group. Moreover, another study by Khozeimeh et al. [2017a] developed an expert system with fuzzy rules, and one such rule for immunotherapy is “If (types of wart is Plantar) and (time elapsed before treatment is VeryLate) then (response to treatment is Yes).” In Khozeimeh et al. [2017a]’s expert system, time elapsed before treatment longer than six months is considered “VeryLate”. This rule echoes the common and unique clusters for the immunotherapy group found by PAM. In the unique clusters 4 and 5, and the common clusters 1 to 3, the time before treatment was 6.96, 7.38, 6.19, 6.71 and 8.63 months, respectively, all larger than six months.

Additional results are illustrated in Figure A.5 in Appendix A.13, which shows the cluster membership of each patient. The figure indicates that patients with a large area of warts are unique to the immunotherapy group, while those with a younger age are mostly

from the cryotherapy group.

7 Discussion

We have introduced a novel Bayesian nonparametric model called PAM that can induce dependent clusters across groups and has a mean process of FSBP. This model allows the weights of clusters to be exactly zero in some groups, effectively removing these clusters from those groups, and generating an interpretable clustering structure. In simulation studies, PAM demonstrated competitive performance, and in the two case studies, it produced sensible results. Our methodology accommodates count data and multivariate observations and follows the efficient slice sampler for CAM, with substantial modifications due to the use of ZAB in our construction.

There are some limitations to our current work. Firstly, the model is unable to cluster groups (i.e., distributional clusters), unlike NDP and CAM. However, we are currently working on a separate model that extends PAM to cluster nested data at both group and observational levels. Secondly, the model has not been applied to real datasets consisting of different types of covariates, such as binary and multinomial covariates. Finally, considering longitudinal data is another interesting direction for extending the model.

References

- Milton Abramowitz, Irene A Stegun, and Robert H Romer. Handbook of mathematical functions with formulas, graphs, and mathematical tables, 1988.
- Mario Beraha, Alessandra Guglielmi, and Fernando A Quintana. The semi-hierarchical dirichlet process and its application to clustering homogeneous distributions. *Bayesian Analysis*, 16(4):1187–1219, 2021.

- Federico Camerlenghi, David B Dunson, Antonio Lijoi, Igor Prünster, and Abel Rodríguez. Latent nested nonparametric priors (with discussion). *Bayesian Analysis*, 14(4):1303–1356, 2019.
- Antonio Canale and David B Dunson. Bayesian kernel mixtures for counts. *Journal of the American Statistical Association*, 106(496):1528–1539, 2011.
- Francesco Denti, Federico Camerlenghi, Michele Guindani, and Antonietta Mira. A common atoms model for the bayesian nonparametric analysis of nested data. *Journal of the American Statistical Association*, pages 1–12, 2021.
- David B Dunson and Ju-Hyun Park. Kernel stick-breaking processes. *Biometrika*, 95(2):307–323, 2008.
- Michael D Escobar and Mike West. Bayesian density estimation and inference using mixtures. *Journal of the american statistical association*, 90(430):577–588, 1995.
- Thomas S Ferguson. A bayesian analysis of some nonparametric problems. *The annals of statistics*, pages 209–230, 1973.
- Chris Fraley and AE Raftery. Mclust: Software for model-based cluster and discriminant analysis. *Department of Statistics, University of Washington: Technical Report*, 342, 1998.
- Daniela Graf, Raffaella Di Cagno, Frida Fåk, Harry J Flint, Margareta Nyman, Maria Saarela, and Bernhard Watzl. Contribution of diet to the composition of the human gut microbiota. *Microbial ecology in health and disease*, 26(1):26164, 2015.
- Roger A Horn and Charles R Johnson. Norms for vectors and matrices. *Matrix analysis*, pages 313–386, 1990.

- Lawrence Hubert and Phipps Arabie. Comparing partitions. *Journal of classification*, 2(1): 193–218, 1985.
- Juan Jovel, Jordan Patterson, Weiwei Wang, Naomi Hotte, Sandra O’Keefe, Troy Mitchel, Troy Perry, Dina Kao, Andrew L Mason, Karen L Madsen, et al. Characterization of the gut microbiome using 16s or shotgun metagenomics. *Frontiers in microbiology*, 7:459, 2016.
- Maria Kalli, Jim E Griffin, and Stephen G Walker. Slice sampling mixture models. *Statistics and computing*, 21(1):93–105, 2011.
- Abhishek Kaul, Siddhartha Mandal, Ori Davidov, and Shyamal D Peddada. Analysis of microbiome data in the presence of excess zeros. *Frontiers in microbiology*, 8:2114, 2017.
- Fahime Khozeimeh, Roohallah Alizadehsani, Mohamad Roshanzamir, Abbas Khosravi, Poursan Layegh, and Saeid Nahavandi. An expert system for selecting wart treatment method. *Computers in biology and medicine*, 81:167–175, 2017a.
- Fahime Khozeimeh, Farahzad Jabbari Azad, Yaghoub Mahboubi Oskouei, Majid Jafari, Shahrzad Tehranian, Roohallah Alizadehsani, and Poursan Layegh. Intralesional immunotherapy compared to cryotherapy in the treatment of warts. *International journal of dermatology*, 56(4):474–478, 2017b.
- Antonio Lijoi, Igor Prünster, and Giovanni Rebaudo. Flexible clustering via hidden hierarchical dirichlet priors. *Scandinavian Journal of Statistics*, 2022.
- J MacQueen. Classification and analysis of multivariate observations. In *5th Berkeley Symp. Math. Statist. Probability*, pages 281–297, 1967.
- Marina Meilă. Comparing clusterings—an information based distance. *Journal of multivariate analysis*, 98(5):873–895, 2007.

- Ramsés H Mena, Matteo Ruggiero, and Stephen G Walker. Geometric stick-breaking processes for continuous-time bayesian nonparametric modeling. *Journal of Statistical Planning and Inference*, 141(9):3217–3230, 2011.
- Jeffrey W Miller. An elementary derivation of the chinese restaurant process from sethuraman’s stick-breaking process. *Statistics & Probability Letters*, 146:112–117, 2019.
- Stephen JD O’Keefe, Jia V Li, Leo Lahti, Junhai Ou, Franck Carbonero, Khaled Mohammed, Joram M Posma, James Kinross, Elaine Wahl, Elizabeth Ruder, et al. Fat, fibre and cancer risk in african americans and rural africans. *Nature communications*, 6(1):1–14, 2015.
- Panagiotis Papastamoulis. label. switching: An r package for dealing with the label switching problem in mcmc outputs. *arXiv preprint arXiv:1503.02271*, 2015.
- Panagiotis Papastamoulis and George Iliopoulos. An artificial allocations based solution to the label switching problem in bayesian analysis of mixtures of distributions. *Journal of Computational and Graphical Statistics*, 19(2):313–331, 2010.
- Jim Pitman. Exchangeable and partially exchangeable random partitions. *Probability theory and related fields*, 102(2):145–158, 1995.
- Jim Pitman. Poisson–dirichlet and gem invariant distributions for split-and-merge transformations of an interval partition. *Combinatorics, Probability and Computing*, 11(5):501–514, 2002.
- Mădălina Preda, Mircea Ioan Popa, Mara Mădălina Mihai, Teodora Cristiana Oțelea, and Alina Maria Holban. Effects of coffee on intestinal microbiota, immunity, and disease. *Caffeinated and Cocoa Based Beverages*, pages 391–421, 2019.

Abel Rodriguez, David B Dunson, and Alan E Gelfand. The nested dirichlet process. *Journal of the American statistical Association*, 103(483):1131–1154, 2008.

Jayaram Sethuraman. A constructive definition of dirichlet priors. *Statistica sinica*, pages 639–650, 1994.

Yee Teh, Michael Jordan, Matthew Beal, and David Blei. Sharing clusters among related groups: Hierarchical dirichlet processes. *Advances in neural information processing systems*, 17, 2004.

Sara Wade and Zoubin Ghahramani. Bayesian cluster analysis: Point estimation and credible balls (with discussion). *Bayesian Analysis*, 13(2):559–626, 2018.

Appendix

A.1 Features of BNP models

Table A.1 summarizes the feature of reviewed BNP models, along with the proposed PAM model.

BNP Models	Common Atoms / Common Weights	Common Atoms / Distinct Weights	Distinct Atoms / Distinct Weights	Plaid* Atoms / Distinct Weights
CAM	✓	✓		
HDP		✓		
LNP	✓			✓
NDP	✓		✓	
PAM		✓	✓	✓

Table A.1: Features supported by various BNP models. A check-mark means the model supports such feature. * : “Plaid” atoms means groups can share common atoms but can also possess unique atoms.

A.2 Proof of Theorem 1

As discussed in Subsection 2.4, the FSBP is a special case of the kernel stick-breaking process of Dunson and Park [2008]. Using their notation, the kernel function $K(\mathbf{x}, \Gamma_k) = \bar{p}$, i.e., constant over k and independent of covariates. Thus, their theoretical results are applicable in our case. From equation (4) of Dunson and Park [2008], the mean of G^* is immediate and given by

$$\mathbb{E}[G^*(A)] = \mathbb{E}[\mathbb{E}[G^*(A)|\boldsymbol{\beta}', \bar{p}]] = \mathbb{E}[H(A)] = H(A),$$

where $\beta' = \{\beta'_k\}_{k=1}^\infty, \beta'_k \sim \text{Beta}(1, \gamma)$. To find the variance of G^* , apply equation (7) of Theorem 1 of Dunson and Park [2008]

$$\text{Var}(G^*(A)) = \frac{\mu^{(2)} \text{Var}_{Q(A)}}{2\mu - \mu^{(2)}} \quad (\text{A.1})$$

where

$$\text{Var}_{Q(A)} = \text{Var}_H\{\delta_{\phi_k}(A)\} = H(A)(1 - H(A)),$$

$$\mu = \bar{p} \text{E}[\beta'_k] = \frac{\bar{p}}{1 + \gamma},$$

and

$$\mu^{(2)} = \bar{p}^2 \text{E}[\beta_k'^2] = \frac{2\bar{p}^2}{(1 + \gamma)(2 + \gamma)}.$$

Substituting the expression for $\text{Var}_{Q(A)}$, $\mu(x)$, and $\mu^{(2)}(x)$ into equation (A.1), we obtain

$$\text{Var}(G^*(A)) = \frac{H(A)(1 - H(A))}{\frac{1+\gamma}{\bar{p}} + \frac{1-\bar{p}}{\bar{p}}}.$$

□

A.3 Proof of Theorem 2

Denote $\Phi = \{\phi_1, \phi_2, \dots\}$ the infinite mixture of point masses in G^* . Consider n samples from G^* , $\Theta = \{\theta_i\}_{i=1}^n, \theta_i | G^* \sim G^*$, and θ_i takes a value in Φ with a probability. Assume there are K clusters, denote the unique values by $\Phi_K = \{\phi_{r_1}, \dots, \phi_{r_K}\}$ where each r_k indexes the k th cluster and $r_k \in \mathbb{N}$. Denote $\nabla = \{r_1, \dots, r_K\}$ the index set of the K clusters. Let $\mathbf{z} = \{z_1, \dots, z_n\}$ be the cluster label where $\{z_i = k\}$ means observation θ_i belongs to cluster k , i.e., $\{\theta_i = \phi_{r_k}\}$. Further, denote $c_k = \{i : z_i = k\}$ the indices of θ_i 's belonging to cluster k . It is important to note that the cluster label k 's do not need to be consecutive integers. For example, $K = 3$ and $\nabla = \{1, 3, 5\}$ or $K = 5$ and $\nabla = \{2, 5, 6, 20, 100\}$. Lastly,

assume the unique value of the k th cluster is ϕ_k , i.e., $\{\theta_i = \phi_k\}$ if $\{z_i = k\}$, for $k \in \nabla$.

Let $m = \max(z_1, \dots, z_n)$. It follows that $K \leq m$ due to the fact that the cluster labels do not need to be consecutive integers. A partition \mathbf{z} of the n samples Θ is then denoted as $C(\mathbf{z}) = \{c_k : k \in \nabla\}$, the collection of c_k 's, where $c_k \cap c_{k'} = \emptyset$ for $k \neq k'$, $|C(\mathbf{z})| = K$, and $\cup_{k \in \nabla} c_k = \{1, \dots, n\}$. Here, $|\cdot|$ refers to the cardinality of a set. The EPPF of G^* evaluated at a specific partition C is given by

$$\Pr(C(\mathbf{z}) = C) = \sum_{\mathbf{z}^* \in \mathbb{N}^n} \Pr(C(\mathbf{z}^*) = C | \mathbf{z} = \mathbf{z}^*) \Pr(\mathbf{z} = \mathbf{z}^*) = \sum_{\mathbf{z}^* \in \mathbb{N}^n} \mathbb{1}(C(\mathbf{z}^*) = C) \Pr(\mathbf{z} = \mathbf{z}^*) \quad (\text{A.2})$$

where \mathbb{N}^n is the n -dimensional space of positive integers. The second equality is true since given $\mathbf{z} = \mathbf{z}^*$, $C(\mathbf{z}^*)$ is fixed and is either equal to C or not.

We first find $\Pr(\mathbf{z} = \mathbf{z}^*)$. For a specific $\mathbf{z}^* = \{z_1^*, \dots, z_n^*\}$, denote $e_k(\mathbf{z}^*) = |\{i : z_i^* = k\}|$, $f_k(\mathbf{z}^*) = |\{i : z_i^* > k\}|$, and $g_k(\mathbf{z}^*) = |\{i : z_i^* \geq k\}|$. Also let $m(\mathbf{z}^*) = \max(z_1^*, \dots, z_n^*)$. Recall the definition of FSBP in Section 2, with $a = b = 1$, $\pi'_k \sim \text{Beta}(1, 1)$, and we have

$$\begin{aligned} \Pr(\mathbf{z} = \mathbf{z}^*) &= \int \Pr(\mathbf{z}^* | \pi'_1, \dots, \pi'_{m(\mathbf{z}^*)}) p(\pi'_1) \cdots p(\pi'_{m(\mathbf{z}^*)}) d\pi'_1 \cdots d\pi'_{m(\mathbf{z}^*)} \\ &= \int \left[\prod_{k=1}^{m(\mathbf{z}^*)} \left\{ \bar{p} \pi'_k \prod_{l < k} (1 - \bar{p} \pi'_l) \right\}^{e_k(\mathbf{z}^*)} \right] p(\pi'_1) \cdots p(\pi'_{m(\mathbf{z}^*)}) d\pi'_1 \cdots d\pi'_{m(\mathbf{z}^*)} \\ &= \int \left[\prod_{k=1}^{m^*} (\bar{p} \pi'_k)^{e_k(\mathbf{z}^*)} (1 - \bar{p} \pi'_k)^{f_k(\mathbf{z}^*)} \right] p(\pi'_1) \cdots p(\pi'_{m(\mathbf{z}^*)}) d\pi'_1 \cdots d\pi'_{m(\mathbf{z}^*)} \\ &= \prod_{k=1}^{m(\mathbf{z}^*)} \left\{ \bar{p}^{g_k(\mathbf{z}^*)} \int \pi'_k{}^{e_k(\mathbf{z}^*)} \left(\frac{1}{\bar{p}} - \pi'_k \right)^{f_k(\mathbf{z}^*)} p(\pi'_k) d\pi'_k \right\}, \end{aligned}$$

where $e_k(\mathbf{z}^*) + f_k(\mathbf{z}^*) = g_k(\mathbf{z}^*)$. Since $p(\pi'_k) = \frac{1}{B(1,1)}(\pi'_k)^{1-1}(1 - \pi'_k)^{1-1} = 1$, we have

$$\Pr(\mathbf{z} = \mathbf{z}^*) = \prod_{k=1}^{m(\mathbf{z}^*)} \bar{p}^{g_k(\mathbf{z}^*)} \int \pi'_k{}^{e_k(\mathbf{z}^*)} \left(\frac{1}{\bar{p}} - \pi'_k\right)^{f_k(\mathbf{z}^*)} d\pi'_k = \prod_{k=1}^{m(\mathbf{z}^*)} \frac{1}{\bar{p}} B_{\bar{p}}(e_k(\mathbf{z}^*)+1, f_k(\mathbf{z}^*)+1)$$

where $B_{\bar{p}}(e_k(\mathbf{z}^*) + 1, f_k(\mathbf{z}^*) + 1)$ is the incomplete beta function. Using the property of incomplete beta function and denoting $I_p(a, b)$ the regularized incomplete beta function, we have

$$\begin{aligned} \Pr(\mathbf{z} = \mathbf{z}^*) &= \prod_{k=1}^{m(\mathbf{z}^*)} \frac{1}{\bar{p}} B_{\bar{p}}(e_k(\mathbf{z}^*) + 1, f_k(\mathbf{z}^*) + 1) \\ &= \prod_{k=1}^{m(\mathbf{z}^*)} \frac{1}{\bar{p}} B(e_k(\mathbf{z}^*) + 1, f_k(\mathbf{z}^*) + 1) I_{\bar{p}}(e_k(\mathbf{z}^*) + 1, f_k(\mathbf{z}^*) + 1) \\ &= \prod_{k=1}^{m(\mathbf{z}^*)} \frac{1}{\bar{p}} \frac{\Gamma(e_k(\mathbf{z}^*) + 1) \Gamma(f_k(\mathbf{z}^*) + 1)}{\Gamma(e_k(\mathbf{z}^*) + f_k(\mathbf{z}^*) + 2)} I_{\bar{p}}(e_k(\mathbf{z}^*) + 1, f_k(\mathbf{z}^*) + 1) \\ &= \prod_{k=1}^{m(\mathbf{z}^*)} \frac{1}{\bar{p}} \frac{\Gamma(e_k(\mathbf{z}^*) + 1) \Gamma(f_k(\mathbf{z}^*) + 1)}{\Gamma(g_k(\mathbf{z}^*) + 2)} I_{\bar{p}}(e_k(\mathbf{z}^*) + 1, f_k(\mathbf{z}^*) + 1) \\ &= \left\{ \prod_{k=1}^{m(\mathbf{z}^*)} \Gamma(e_k(\mathbf{z}^*) + 1) \right\} \left\{ \prod_{k=1}^{m(\mathbf{z}^*)} \frac{1}{\bar{p}(g_k(\mathbf{z}^*) + 1)} \right\} \left\{ \prod_{k=1}^{m(\mathbf{z}^*)} \frac{\Gamma(g_{k+1}(\mathbf{z}^*) + 1)}{\Gamma(g_k(\mathbf{z}^*) + 1)} I_{\bar{p}}(e_k(\mathbf{z}^*) + 1, f_k(\mathbf{z}^*) + 1) \right\} \\ &= \left\{ \prod_{c \in C(\mathbf{z}^*)} \Gamma(|c| + 1) \right\} \left\{ \prod_{k=1}^{m(\mathbf{z}^*)} \frac{1}{\bar{p}(g_k(\mathbf{z}^*) + 1)} \right\} \left\{ \frac{1}{\Gamma(n + 1)} \prod_{k=1}^{m(\mathbf{z}^*)} I_{\bar{p}}(e_k(\mathbf{z}^*) + 1, f_k(\mathbf{z}^*) + 1) \right\} \end{aligned} \tag{A.3}$$

where $f_k(\mathbf{z}^*) = g_{k+1}(\mathbf{z}^*)$, $g_1(\mathbf{z}^*) = n$, and $g_{m(\mathbf{z}^*)+1}(\mathbf{z}^*) = 0$.

Next, we use the following relationship between the CDF of a binomial distribution and the regularized incomplete beta function. Denote $F(k; n, 1 - p)$ the CDF of a binomial distribution with k the number of success, n the sample size, and $(1 - p)$ the success

probability. Then, it follows that

$$F(k; n, 1 - p) = I_p(n - k, k + 1),$$

which can be seen from consecutively apply integration by parts to the regularized incomplete beta function as follows:

$$\begin{aligned} I_p(n - k, k + 1) &= \frac{\int_0^p t^{n-k-1}(1-t)^k dt}{B(n - k, k + 1)} = \frac{n!}{(n - k - 1)!k!} \int_0^p t^{n-k-1}(1-t)^k dt \\ &= (n - k) \frac{n!}{(n - k)!k!} \int_0^p t^{n-k-1}(1-t)^k dt = (n - k) \binom{n}{k} \int_0^p t^{n-k-1}(1-t)^k dt \\ &= (n - k) \binom{n}{k} \frac{1}{(n - k)} \left[(1 - p)^k p^{n-k} + k \int_0^p t^{n-k}(1-t)^{k-1} dt \right] \\ &= \binom{n}{k} (1 - p)^k (1 - (1 - p))^{n-k} + k \binom{n}{k} \int_0^p t^{n-k}(1-t)^{k-1} dt = \dots \\ &= \sum_{l=0}^k \binom{n}{l} (1 - p)^l (1 - (1 - p))^{n-l} = F(k; n, 1 - p). \end{aligned}$$

Using the property, we have

$$I_{\bar{p}}(e_k(\mathbf{z}^*) + 1, f_k(\mathbf{z}^*) + 1) = F(f_k(\mathbf{z}^*); g_k(\mathbf{z}^*) + 1, 1 - \bar{p}) = F(g_{k+1}(\mathbf{z}^*); g_k(\mathbf{z}^*) + 1, 1 - \bar{p}).$$

Back to equation (A.2) and substituting in equation (A.3), we have

$$\begin{aligned} \Pr(C(\mathbf{z}) = C) &= \sum_{\mathbf{z}^* \in \mathbb{N}^n} \mathbb{1}(C(\mathbf{z}^*) = C) \left\{ \prod_{c \in C(\mathbf{z}^*)} \Gamma(|c| + 1) \right\} \left\{ \prod_{k=1}^{m(\mathbf{z}^*)} \frac{1}{\bar{p}(g_k(\mathbf{z}^*) + 1)} \right\} \times \\ &\quad \left\{ \frac{1}{\Gamma(n + 1)} \prod_{k=1}^{m(\mathbf{z}^*)} F(g_{k+1}(\mathbf{z}^*); g_k(\mathbf{z}^*) + 1, 1 - \bar{p}) \right\} \end{aligned}$$

$$= \frac{1}{\Gamma(n+1)} \left\{ \prod_{c \in C} \Gamma(|c|+1) \right\} \sum_{\mathbf{z}^* \in \mathbb{N}^n} \mathbb{1}(C(\mathbf{z}^*) = C) \underbrace{\left\{ \underbrace{\prod_{k=1}^{m(\mathbf{z}^*)} \frac{F(g_{k+1}(\mathbf{z}^*); g_k(\mathbf{z}^*) + 1, 1 - \bar{p})}{\bar{p}(g_k(\mathbf{z}^*) + 1)}}_{(A)} \right\}}_{(B)}$$
(A.4)

Now, recall $K = |C|$ is the number of unique clusters in the n samples, and $C = \{c_1, \dots, c_K\}$. Denote S_K the set of all $K!$ permutations of $\{1, \dots, K\}$, and denote $\boldsymbol{\lambda} = \{\lambda_1, \dots, \lambda_K\} \in S_K$ a permutation of $\{1, \dots, K\}$. For any $\boldsymbol{\lambda} \in S_K$, define $\alpha_k(\boldsymbol{\lambda}) = |c_{\lambda_k}| + \dots + |c_{\lambda_K}|$. By definition, $\alpha_{K+1}(\boldsymbol{\lambda}) = 0$. Consider a given \mathbf{z}^* such that $C(\mathbf{z}^*) = C$, recall that r_1, \dots, r_K are the distinct values of \mathbf{z}^* in ascending order, i.e., $r_1 < r_2 < \dots < r_k < \dots < r_K$, $r_k \in \mathbb{N}$, we can rewrite the (A) term in (A.4) as

$$\begin{aligned} \prod_{k=1}^{m(\mathbf{z}^*)} \frac{F(g_{k+1}(\mathbf{z}^*); g_k(\mathbf{z}^*) + 1, 1 - \bar{p})}{\bar{p}(g_k(\mathbf{z}^*) + 1)} &= \left(\frac{F(g_{r_1}(\mathbf{z}^*); g_{r_1}(\mathbf{z}^*) + 1, 1 - \bar{p})}{\bar{p}(g_{r_1}(\mathbf{z}^*) + 1)} \right)^{r_1} \times \\ &\left(\frac{F(g_{r_2}(\mathbf{z}^*); g_{r_2}(\mathbf{z}^*) + 1, 1 - \bar{p})}{\bar{p}(g_{r_2}(\mathbf{z}^*) + 1)} \right)^{r_2 - r_1} \times \dots \times \left(\frac{F(g_{r_K}(\mathbf{z}^*); g_{r_K}(\mathbf{z}^*) + 1, 1 - \bar{p})}{\bar{p}(g_{r_K}(\mathbf{z}^*) + 1)} \right)^{r_K - r_{K-1}} \\ &= \left(\frac{F(\alpha_2(\boldsymbol{\lambda}); \alpha_1(\boldsymbol{\lambda}) + 1, 1 - \bar{p})}{\bar{p}(\alpha_1(\boldsymbol{\lambda}) + 1)} \right)^{d_1} \times \left(\frac{F(\alpha_3(\boldsymbol{\lambda}); \alpha_2(\boldsymbol{\lambda}) + 1, 1 - \bar{p})}{\bar{p}(\alpha_2(\boldsymbol{\lambda}) + 1)} \right)^{d_2} \times \dots \times \\ &\left(\frac{F(\alpha_{K+1}(\boldsymbol{\lambda}); \alpha_K(\boldsymbol{\lambda}) + 1, 1 - \bar{p})}{\bar{p}(\alpha_K(\boldsymbol{\lambda}) + 1)} \right)^{d_K} = \prod_{k=1}^K \left(\frac{F(\alpha_{k+1}(\boldsymbol{\lambda}); \alpha_k(\boldsymbol{\lambda}) + 1, 1 - \bar{p})}{\bar{p}(\alpha_k(\boldsymbol{\lambda}) + 1)} \right)^{d_k} \end{aligned}$$

where $\mathbf{d} = (d_1, \dots, d_K)$, $d_1 = r_k$, and $d_k = r_k - r_{k-1}$ for $k = 2, \dots, K$. For any $\mathbf{z}^* \in \mathbb{N}^n$, notice that the definition of \mathbf{d} and $\boldsymbol{\lambda}$ sets up a one-to-one correspondence, which is a bijection, between $\{\mathbf{z}^* \in \mathbb{N}^n : C(\mathbf{z}^*) = C\}$ and $\{(\boldsymbol{\lambda}, \mathbf{d}) : \boldsymbol{\lambda} \in S_K, \mathbf{d} \in \mathbb{N}^K\}$, and the

expression in (B) in (A.4) can then be rewritten as

$$\begin{aligned}
& \sum_{\mathbf{z}^* \in \mathbb{N}^n} 1(C(\mathbf{z}^*) = C) \left\{ \prod_{k=1}^{m(\mathbf{z}^*)} \frac{F(g_{k+1}(\mathbf{z}^*); g_k(\mathbf{z}^*) + 1, 1 - \bar{p})}{\bar{p}(g_k(\mathbf{z}^*) + 1)} \right\} \\
& \stackrel{(a)}{=} \sum_{\boldsymbol{\lambda} \in S_K} \sum_{\mathbf{d} \in \mathbb{N}^K} \prod_{k=1}^K \left(\frac{F(\alpha_{k+1}(\boldsymbol{\lambda}); \alpha_k(\boldsymbol{\lambda}) + 1, 1 - \bar{p})}{\bar{p}(\alpha_k(\boldsymbol{\lambda}) + 1)} \right)^{d_k} \\
& = \sum_{\boldsymbol{\lambda} \in S_K} \prod_{k=1}^K \sum_{d_k \in \mathbb{N}} \left(\frac{F(\alpha_{k+1}(\boldsymbol{\lambda}); \alpha_k(\boldsymbol{\lambda}) + 1, 1 - \bar{p})}{\bar{p}(\alpha_k(\boldsymbol{\lambda}) + 1)} \right)^{d_k} \\
& \stackrel{(b)}{=} \sum_{\boldsymbol{\lambda} \in S_K} \prod_{k=1}^K \left\{ \frac{F(\alpha_{k+1}(\boldsymbol{\lambda}); \alpha_k(\boldsymbol{\lambda}) + 1, 1 - \bar{p})}{\bar{p}(\alpha_k(\boldsymbol{\lambda}) + 1) - F(\alpha_{k+1}(\boldsymbol{\lambda}); \alpha_k(\boldsymbol{\lambda}) + 1, 1 - \bar{p})} \right\} \\
& = \sum_{\boldsymbol{\lambda} \in S_K} \prod_{k=1}^K \{\xi_k \cdot (\alpha_k(\boldsymbol{\lambda}) + 1) - 1\}^{-1} \tag{A.5}
\end{aligned}$$

where

$$\xi_k = \frac{\bar{p}}{F(\alpha_{k+1}(\boldsymbol{\lambda}); \alpha_k(\boldsymbol{\lambda}) + 1, 1 - \bar{p})}.$$

The second equality (a) can be shown as the follows: let $f(k, d_k) = \left(\frac{F(\alpha_{k+1}(\boldsymbol{\lambda}); \alpha_k(\boldsymbol{\lambda}) + 1, 1 - \bar{p})}{\bar{p}(\alpha_k(\boldsymbol{\lambda}) + 1)} \right)^{d_k}$, then

$$\begin{aligned}
& \sum_{\mathbf{d} \in \mathbb{N}^K} \prod_{k=1}^K f(k, d_k) = \sum_{d_1 \in \mathbb{N}} \cdots \sum_{d_K \in \mathbb{N}} f(1, d_1) \cdots f(K, d_K) \\
& = \left\{ \sum_{d_1 \in \mathbb{N}} \cdots \sum_{d_{K-1} \in \mathbb{N}} f(1, d_1) \cdots f(K-1, d_{K-1}) \right\} \left(\sum_{d_K \in \mathbb{N}} f(K, d_K) \right) \\
& = \left(\sum_{d_1 \in \mathbb{N}} f(1, d_1) \right) \times \cdots \times \left(\sum_{d_K \in \mathbb{N}} f(K, d_K) \right) = \prod_{k=1}^K \sum_{d_k \in \mathbb{N}} f(k, d_k).
\end{aligned}$$

And the second to the last equality (b) of equation (A.5) is due to geometric sequence.

Substituting this expression into (B) of (A.4), we have proved the EPPF of Theorem 2.

Lastly, for the claim of the EPPF of G^* converging to the EPPF of $G_0 \sim DP(1, H)$ when $\bar{p} \rightarrow 1$, Miller [2019] shows that (Proof of Theorem 2.1 therein) the EPPF of $G_0 \sim DP(1, H)$ can be written as

$$\Pr(C(\mathbf{z}) = C) = \frac{1}{\Gamma(n+1)} \left\{ \prod_{c \in C} \Gamma(|c|) \right\} \left\{ \prod_{c \in C} |c| \right\} \sum_{\boldsymbol{\lambda} \in S_K} \prod_{k=1}^K \left(\frac{1}{\alpha_k(\boldsymbol{\lambda})} \right) = \frac{1}{\Gamma(n+1)} \left\{ \prod_{c \in C} \Gamma(|c|) \right\}. \quad (\text{A.6})$$

When $\bar{p} \rightarrow 1$, $F(\alpha_{k+1}(\boldsymbol{\lambda}); \alpha_k(\boldsymbol{\lambda}) + 1, 0) = 1$ for all k and $\boldsymbol{\lambda} \in S_K$. Thus, we have

$$\lim_{\bar{p} \rightarrow 1} \frac{\bar{p}}{F(\alpha_{k+1}(\boldsymbol{\lambda}); \alpha_k(\boldsymbol{\lambda}) + 1, 1 - \bar{p})} \rightarrow 1,$$

and equation (A.5) reduced to

$$\sum_{\boldsymbol{\lambda} \in S_K} \prod_{k=1}^K \left(\frac{1}{\alpha_k(\boldsymbol{\lambda})} \right).$$

When combined to the first two terms in equation (A.4), we arrive at equation (A.6), which is equal to the EPPF of $G_0 \sim DP(1, H)$. \square

A.4 Proof Lemma 1

Since $G^* \sim FSBP(\bar{p}, \gamma, H)$, consider the following prediction rule for samples $\boldsymbol{\theta}_i | \boldsymbol{\theta}_1, \dots, \boldsymbol{\theta}_{i-1}$, where $\boldsymbol{\theta}_1, \dots, \boldsymbol{\theta}_i | G^* \sim G^*$:

$$\Pr(\boldsymbol{\theta}_i | \boldsymbol{\theta}_1, \dots, \boldsymbol{\theta}_{i-1}) = W_{\text{base}_i} H + \sum_{l=1}^{i-1} W_l \delta_{\boldsymbol{\theta}_l}$$

where W_{base_i} corresponds to the probability $\boldsymbol{\theta}_i$ sampled from the base probability measure H (and not equal to any $\boldsymbol{\theta}_l \in \{\boldsymbol{\theta}_1, \dots, \boldsymbol{\theta}_{i-1}\}$) where there is i samples, and W_l corresponds to the probability of $\boldsymbol{\theta}_i$ sampled from a previously seen $\boldsymbol{\theta}_l$ for $l = 1, \dots, i-1$. Then, we

have

$$\Pr(w_i = 1 | \bar{p}, \gamma) = \Pr(\boldsymbol{\theta}_i \notin \{\boldsymbol{\theta}_1, \dots, \boldsymbol{\theta}_{i-1}\} | G^*) = W_{\text{base}_i}.$$

W_{base_i} can be evaluated by (using the prediction rule in Theorem 2 of Dunson and Park [2008])

$$W_{\text{base}_i} = \left\{ 1 - \sum_{k=2}^i (-1)^k \sum_{I \in N_i^{(k,i)}} \omega_I \right\},$$

where $N_i^{(k,i)}$ is a set contains all possible k -dimensional subsets of $\{1, \dots, i\}$ that includes index i , with I an element (a set) in the set, $\omega_I = \mu_I \cdot \left(\sum_{l=1}^{|I|} (-1)^{l-1} \sum_{m \in I_l} \mu_m \right)^{-1}$, $\mu_I = E[\prod_{k \in I} \bar{p} \pi_k']$, and I_l the set of length- l subsets of the set I . The cardinality of the sets $N_i^{(k,i)}$, I , and I_l are $|N_i^{(k,i)}| = \binom{i-1}{k-1}$, $|I| = k$, and $|I_l| = \binom{k}{l}$, respectively. For example, let $i = 3$, $k = 2$, and $l = 1$. $N_{i=3}^{(k=2,i=3)} = \{I_1, I_2\} = \{\{1, 3\}, \{2, 3\}\}$, with $|N_{i=3}^{(k=2,i=3)}| = 2$. Also, $|I_1| = |I_2| = 2$. And when $I = I_1$, $I_{l=1} = \{\{1\}, \{3\}\}$, and when $I = I_2$, $I_{l=1} = \{\{2\}, \{3\}\}$. Both have cardinality $|I_{l=1}| = 2$.

For G^* , recall $\pi_k' \sim \text{Beta}(1, \gamma)$. For a set I , $\mu_I = E[\prod_{k \in I} \bar{p} \pi_k']$, which can be shown to be

$$\mu_I = \bar{p}^{|I|} \prod_{l=1}^{|I|} \frac{l}{l + \gamma}.$$

Thus, μ_I depends on the cardinality of the set I only. Furthermore, for $\sum_{m \in I_l} \mu_m$ in the denominator of ω_I , μ_m can be similarly computed, and the values are the same for all $m \in I_l$ (since μ_m depends only on $|m|$, and all $m \in I_l$ are of the same cardinality that is equal to l). Plugging in μ_I and $\sum_{m \in I_l} \mu_m$ to the theorem, we have

$$\omega_I = \frac{\bar{p}^{|I|} \prod_{l=1}^{|I|} \frac{l}{l + \gamma}}{\sum_{l=1}^{|I|} (-1)^{l-1} \binom{|I|}{l} \bar{p}^l \prod_{m=1}^l \frac{m}{m + \gamma}},$$

which again only depends on the cardinality of the set I , i.e., $|I|$. Let $|N_i^{(k,i)}| = \binom{i-1}{k-1} =$

B. Further notice that the sets in $N_i^{(k,i)}$, denoted as $I_1, \dots, I_{b'}, \dots, I_B$, have the same cardinality for a given k , i.e., $|I_{b'}| = k$ for all $b' \in \{1, \dots, B\}$. Thus, we have

$$\begin{aligned}
W_{\text{base}_i} &= 1 - \sum_{k=2}^i (-1)^k \sum_{I \in N_i^{(k,i)}} \omega_I = 1 - \sum_{k=2}^i (-1)^k \binom{i-1}{k-1} \frac{\bar{p}^k \prod_{l=1}^k \frac{l}{l+\gamma}}{\sum_{l=1}^k (-1)^{l-1} \binom{k}{l} \bar{p}^l \prod_{m=1}^l \frac{m}{m+\gamma}} \\
&= 1 - \sum_{k=2}^i (-1)^k \binom{i-1}{k-1} \frac{k!}{\prod_{l=1}^k (l+\gamma)} \frac{\bar{p}^{k-1}}{\sum_{l=1}^k (-1)^{l-1} \binom{k}{l} \bar{p}^{l-1} \frac{l!}{\prod_{m=1}^l (m+\gamma)}} \\
&= 1 - \sum_{k=2}^i (-1)^k \binom{i-1}{k-1} \frac{k!}{\prod_{l=1}^k (l+\gamma)} \frac{(\gamma+1) \bar{p}^{k-1}}{k \times {}_2F_1(1, 1-k; \gamma+2; \bar{p})} \\
&= 1 - \sum_{k=2}^i (-1)^k \binom{i-1}{k-1} \frac{(k-1)!}{\prod_{l=1}^k (l+\gamma)} \frac{(\gamma+1) \bar{p}^{k-1}}{{}_2F_1(1, 1-k; \gamma+2; \bar{p})}. \tag{A.7}
\end{aligned}$$

where ${}_2F_1(a, b; c; z)$ is the hypergeometric function. \square

A.5 Proof Lemma 2

Setting let $\bar{p} = 1$ in equation (A.7), we have

$$\begin{aligned}
\Pr(w_i = 1 | \bar{p} = 1, \gamma) &= 1 - \sum_{k=2}^i (-1)^k \binom{i-1}{k-1} \frac{(k-1)!}{\prod_{l=1}^k (l+\gamma)} \frac{(\gamma+1)}{{}_2F_1(1, 1-k; \gamma+2; 1)} \\
&\stackrel{(a)}{=} 1 - \sum_{k=2}^i (-1)^k \binom{i-1}{k-1} \frac{(k-1)!}{\prod_{l=1}^k (l+\gamma)} \frac{(\gamma+1)}{\frac{\gamma+1}{\gamma+k}} \\
&= 1 - \sum_{k=2}^i (-1)^k \frac{\Gamma(i)}{\Gamma(i-k+1)} \frac{\Gamma(\gamma+1)}{\Gamma(\gamma+k)} = 1 - \frac{i-1}{\gamma+i-1} = \frac{\gamma}{\gamma+i-1},
\end{aligned}$$

where the second equality (a) is because

$${}_2F_1(1, 1 - k; \gamma + 2; 1) = \frac{\Gamma(\gamma + 2)\Gamma(\gamma + k)}{\Gamma(\gamma + 1)\Gamma(\gamma + 1 + k)} = \frac{(\gamma + 1)\Gamma(\gamma + 1)\Gamma(\gamma + k)}{\Gamma(\gamma + 1)(\gamma + k)\Gamma(\gamma + k)} = \frac{\gamma + 1}{\gamma + k}.$$

Notice that $\frac{\gamma}{\gamma+i-1}$ is the probability of generating a new sample $\boldsymbol{\theta}_i \notin \{\boldsymbol{\theta}_1, \dots, \boldsymbol{\theta}_{i-1}\}$, i.e., from the base measure, in DP. \square

A.6 Proof Theorem 3

To show $\Pr(w_i = 1 | \bar{p}, \gamma) \geq \frac{\gamma}{\gamma+i-1}$, it is sufficient to show that $1 - \frac{\gamma}{\gamma+i-1} \geq 1 - \Pr(w_i = 1 | \bar{p}, \gamma)$, or

$$\frac{i-1}{\gamma+i-1} \geq \sum_{k=2}^i (-1)^k \binom{i-1}{k-1} \frac{(k-1)!}{\prod_{l=1}^k (l+\gamma)} \frac{(\gamma+1)\bar{p}^{k-1}}{{}_2F_1(1, 1-k; \gamma+2; \bar{p})}.$$

First, notice that the hypergeometric function ${}_2F_1(1, 1-k; \gamma+2; \bar{p})$ is monotonically decreasing with respect to \bar{p} since

$$\begin{aligned} \frac{d}{d\bar{p}} {}_2F_1(1, 1-k; \gamma+2; \bar{p}) &= -\frac{(k-1){}_2F_1(2, 2-k; \gamma+3; \bar{p})}{\gamma+2} \\ &= -\frac{(k-1)(1-\bar{p})^{\gamma+k-1} {}_2F_1(\gamma+1, \gamma+k+1; \gamma+3; \bar{p})}{\gamma+2} < 0, \end{aligned}$$

with ${}_2F_1(1, 1-k; \gamma+2; 0) = 1$ and ${}_2F_1(1, 1-k; \gamma+2; 1) = \frac{\gamma+1}{\gamma+k}$. As a result, $\frac{1}{{}_2F_1(1, 1-k; \gamma+2; \bar{p})}$ is monotonically increasing with \bar{p} , with maximum at $\bar{p} = 1$, and

$$\lim_{\bar{p} \rightarrow 1} \frac{1}{{}_2F_1(1, 1-k; \gamma+2; \bar{p})} = \frac{\gamma+k}{\gamma+1}.$$

Next, when substituting the maximum for ${}_2F_1(1, 1-k; \gamma+2; \bar{p})$, it can be shown that

$$\frac{i-1}{\gamma+i-1} - \sum_{k=2}^i (-1)^k \binom{i-1}{k-1} \frac{(k-1)!}{\prod_{l=1}^k (l+\gamma)} \frac{(\gamma+1)\bar{p}^{k-1}}{{}_2F_1(1, 1-k; \gamma+2; \bar{p})}$$

$$\begin{aligned}
&\geq \frac{i-1}{\gamma+i-1} - \sum_{k=2}^i (-1)^k \binom{i-1}{k-1} \frac{(k-1)!}{\prod_{l=1}^k (l+\gamma)} \frac{(\gamma+1)\bar{p}^{k-1}(\gamma+k)}{\gamma+1} \\
&= \frac{i-1}{\gamma+i-1} - \sum_{k=2}^i (-1)^k \frac{\Gamma(i)}{\Gamma(i-k+1)} \frac{\Gamma(\gamma+1)}{\Gamma(\gamma+k)} \bar{p}^{k-1} \\
&= \frac{i-1}{\gamma+i-1} - \frac{(i-1) {}_2F_1(1, 2-i; \gamma+2; \bar{p}) \bar{p}}{\gamma+1}.
\end{aligned}$$

Now, for $\bar{p} \cdot {}_2F_1(1, 2-i; \gamma+2; \bar{p})$, from the property of hypergeometric function, we have $0 \cdot {}_2F_1(1, 2-i; \gamma+2; 0) = 0 \cdot 1 = 0$, and $1 \cdot {}_2F_1(1, 2-i; \gamma+2; 1) = \frac{\Gamma(\gamma+2)\Gamma(\gamma+i-1)}{\Gamma(\gamma+1)\Gamma(\gamma+i)} = \frac{\gamma+1}{\gamma+i-1}$. In addition, we have

$$\begin{aligned}
&\frac{d}{d\bar{p}} {}_2F_1(1, 2-i; \gamma+2; \bar{p}) \bar{p} = {}_2F_1(2, 2-i; \gamma+2; \bar{p}) \\
&= (1-\bar{p})^{\gamma+i-2} {}_2F_1(\gamma, \gamma+i; \gamma+2; \bar{p}) > 0,
\end{aligned}$$

and therefore, $\bar{p} \cdot {}_2F_1(1, 2-i; \gamma+2; \bar{p})$ monotonically increases with \bar{p} , is equal to 0 if $\bar{p} = 0$, and is equal to $\frac{\gamma+1}{\gamma+i-1}$ if $\bar{p} = 1$. Consequently, for $\bar{p} \in (0, 1]$, we have

$$\frac{i-1}{\gamma+i-1} - \frac{(i-1) {}_2F_1(1, 2-i; \gamma+2; \bar{p}) \bar{p}}{\gamma+1} \geq \frac{i-1}{\gamma+i-1} - \frac{i-1}{\gamma+i-1} = 0.$$

□

A.7 Proof of Proposition 1

We first show the second claim in the proposition. Writing G_j in a stick-breaking form and taking expectation w.r.t π_{jk} , conditional on $\beta = \{\beta_k\}_{k=1}^\infty$ and p_j , from equation (3), we have

$$E[\pi'_{jk}|\boldsymbol{\beta}, p_j] = \frac{p_j\beta_k}{1 - \sum_{l=1}^{k-1} \beta_l}. \quad (\text{A.8})$$

Then

$$\begin{aligned} E[E[\pi_{jk}|\boldsymbol{\beta}, p_j]] &= E \left[E \left[\pi'_{jk} \prod_{l=1}^{k-1} (1 - \pi'_{jl}) | \boldsymbol{\beta}, p_j \right] \right] \\ &= E \left[\frac{p_j\beta_k}{1 - \sum_{l=1}^{k-1} \beta_l} \prod_{l=1}^{k-1} \left(\frac{1 - \sum_{w=1}^{l-1} \beta_w - p_j\beta_l}{1 - \sum_{w=1}^{l-1} \beta_w} \right) \right] \\ &= E \left[p_j\beta_k \prod_{l=1}^{k-1} \left(\frac{1 - \sum_{w=1}^{l-1} \beta_w - p_j\beta_l}{1 - \sum_{w=1}^l \beta_w} \right) \right] \\ &= E \left[p_j\beta_k \prod_{l=1}^{k-1} \left\{ \frac{\sum_{w=l+1}^{\infty} \beta_w + (1 - p_j)\beta_l}{\sum_{w=l+1}^{\infty} \beta_w} \right\} \right] \\ &= E \left[p_j\beta_k \prod_{l=1}^{k-1} \left\{ 1 + \frac{(1 - p_j)\beta_l}{\sum_{w=l+1}^{\infty} \beta_w} \right\} \right] \end{aligned}$$

Expanding the term in the expectation, we have

$$\begin{aligned} p_j\beta_k \prod_{l=1}^{k-1} \left\{ 1 + \frac{(1 - p_j)\beta_l}{\sum_{w=l+1}^{\infty} \beta_w} \right\} &= p_j\beta'_k \prod_{l=1}^{k-1} (1 - \beta'_l) \prod_{l=1}^{k-1} \left\{ 1 + \frac{(1 - p_j)\beta'_l \prod_{s=1}^{l-1} (1 - \beta'_s)}{\sum_{w=l+1}^{\infty} \beta'_w \prod_{s=1}^{w-1} (1 - \beta'_s)} \right\} \\ &= p_j\beta'_k \prod_{l=1}^{k-1} (1 - \beta'_l) \prod_{l=1}^{k-1} \left\{ 1 + \frac{(1 - p_j)\beta'_l \prod_{s=1}^{l-1} (1 - \beta'_s)}{\beta'_{l+1} \prod_{s=1}^l (1 - \beta'_s) + \beta'_{l+2} \prod_{s=1}^{l+1} (1 - \beta'_s) + \beta'_{l+3} \prod_{s=1}^{l+2} (1 - \beta'_s) + \dots} \right\} \\ &= p_j\beta'_k \prod_{l=1}^{k-1} (1 - \beta'_l) \prod_{l=1}^{k-1} \left\{ 1 + \frac{(1 - p_j)\beta'_l}{\beta'_{l+1} (1 - \beta'_l) + \beta'_{l+2} \prod_{s=l}^{l+1} (1 - \beta'_s) + \beta'_{l+3} \prod_{s=l}^{l+2} (1 - \beta'_s) + \dots} \right\} \end{aligned}$$

$$\begin{aligned}
&= p_j \beta'_k \prod_{l=1}^{k-1} (1 - \beta'_l) \prod_{l=1}^{k-1} \left\{ 1 + \frac{(1 - p_j) \beta'_l}{(1 - \beta'_l)} \frac{1}{\beta'_{l+1} + \beta'_{l+2} (1 - \beta'_{l+1}) + \beta'_{l+3} \prod_{s=l+1}^{l+2} (1 - \beta'_s) + \dots} \right\} \\
&= p_j \beta'_k \prod_{l=1}^{k-1} (1 - \beta'_l) \prod_{l=1}^{k-1} \left\{ 1 + \frac{(1 - p_j) \beta'_l}{(1 - \beta'_l)} \frac{1}{\sum_{w=l+1}^{\infty} \beta'_w \prod_{s=l+1}^{w-1} (1 - \beta'_s)} \right\} \quad (\text{A.9})
\end{aligned}$$

Denote $\Gamma = \sum_{w=l+1}^{\infty} \beta'_w \prod_{s=l+1}^{w-1} (1 - \beta'_s)$ in (A.9). Then it follows

$$1 - \Gamma = (1 - \beta'_{l+1})(1 - \beta'_{l+2}) \cdots = \prod_{w=l+1}^{\infty} (1 - \beta'_w) = 0. \quad (\text{A.10})$$

Therefore, $\Gamma = 1$ and (A.9) becomes

$$\begin{aligned}
E[E[\pi_{j,k} | \boldsymbol{\beta}, p_j]] &= E \left[p_j \beta'_k \prod_{l=1}^{k-1} (1 - \beta'_l) \prod_{l=1}^{k-1} \left\{ \frac{1 - \beta'_l + (1 - p_j) \beta'_l}{(1 - \beta'_l)} \right\} \right] \\
&= E \left[p_j \beta'_k \prod_{l=1}^{k-1} (1 - p_j \beta'_l) \right] = E[p_j] E[\beta'_k] \prod_{l=1}^{k-1} (1 - E[p_j] E[\beta'_l]) \quad (\text{A.11})
\end{aligned}$$

Since $\beta'_k \sim \text{Beta}(1, \gamma)$ and $p_j \sim \text{Beta}(a, b)$, we have

$$E[\pi_{j,k}] = \frac{\bar{p}}{1 + \gamma} \left(\frac{1 + \gamma - \bar{p}}{1 + \gamma} \right)^{k-1} = \frac{1}{1 + \gamma'} \left(\frac{\gamma'}{1 + \gamma'} \right)^{k-1} \quad (\text{A.12})$$

where $\gamma' = \frac{1 + \gamma - \bar{p}}{\bar{p}}$, $\bar{p} = \frac{a}{a+b}$. This proves the second claim in Proposition 1.

To show the first claim, G_j is a proper distribution, i.e., $\sum_{k \geq 1} \pi_{j,k} = 1$, we first show $E \left[\sum_{k \geq 1} \pi_{j,k} \right] = 1$. Notice that

$$\begin{aligned}
E \left[\sum_{k \geq 1} \pi_{j,k} \right] &= \sum_{k \geq 1} E[\pi_{j,k}] = \sum_{k \geq 1} \frac{\bar{p}}{1 + \gamma} \left(\frac{1 + \gamma - \bar{p}}{1 + \gamma} \right)^{k-1} \\
&= \sum_{k^* \geq 0} \frac{\bar{p}}{1 + \gamma} \left(1 - \frac{\bar{p}}{1 + \gamma} \right)^{k^*} = \frac{\bar{p}}{1 + \gamma} \times \frac{1 + \gamma}{\bar{p}} = 1.
\end{aligned}$$

Next, we show $0 < \sum_{k \geq 1} \pi_{j,k} \leq 1$. It is trivial to see that $\sum_{k \geq 1} \pi_{j,k} > 0$. We now show $\sum_{k \geq 1} \pi_{j,k} \leq 1$. Notice

$$1 - \sum_{k \geq 1} \pi_{j,k} = 1 - \pi'_{j,1} - \pi'_{j,2}(1 - \pi'_{j,1}) - \pi'_{j,3}(1 - \pi'_{j,1})(1 - \pi'_{j,2}) - \cdots = \prod_{k=1}^{\infty} (1 - \pi'_{j,k}) \geq 0$$

since $0 \leq \pi'_{j,k} < 1$. Therefore, $\sum_{k \geq 1} \pi_{j,k} \leq 1$. Thus, we have shown $0 < \sum_{k \geq 1} \pi_{j,k} \leq 1$ and $E \left[\sum_{k \geq 1} \pi_{j,k} \right] = 1$, and we conclude $\sum_{k \geq 1} \pi_{j,k} = 1$ almost surely. This proves the first claim of Proposition 1. \square

A.8 Proof of Proposition 2

Let $\boldsymbol{\theta}_{i,1}|G_1 \sim G_1$ and $\boldsymbol{\theta}_{i',2}|G_2 \sim G_2$, without loss of generality,

$$\Pr(\boldsymbol{\theta}_{i,1} = \boldsymbol{\theta}_{i',2}) = \int \Pr(\boldsymbol{\theta}_{i,1} = \boldsymbol{\theta}_{i',2}|G_1, G_2)p(G_1)p(G_2)dG_1dG_2 > \int 0p(G_1)p(G_2)dG_1dG_2 = 0$$

if and only if $\Pr(\boldsymbol{\theta}_{i,1} = \boldsymbol{\theta}_{i',2}|G_1, G_2) > 0$. We next show $\Pr(\boldsymbol{\theta}_{i,1} = \boldsymbol{\theta}_{i',2}|G_1, G_2) > 0$. Denote the set $A^s = \{\phi_k : \pi_{j,k} \neq 0 \text{ and } \pi_{j',k} \neq 0\}$ and $A^j = \{\phi_k : \pi_{j,k} \neq 0\}$ for $j \neq j'$, $j = 1, 2$. Then

$$\Pr(\boldsymbol{\theta}_{i,1} = \boldsymbol{\theta}_{i',2}|G_1, G_2) = \Pr(\boldsymbol{\theta}_{i,1} = \boldsymbol{\theta}_{i',2}|\boldsymbol{\theta}_{i,1} \in A^s, \boldsymbol{\theta}_{i',2} \in A^s)\Pr(\boldsymbol{\theta}_{i,1} \in A^s, \boldsymbol{\theta}_{i',2} \in A^s|G_1, G_2) \quad (\text{A.13})$$

The second term (A.13) is

$$\begin{aligned} & \Pr(\boldsymbol{\theta}_{i,1} \in A^s, \boldsymbol{\theta}_{i',2} \in A^s|G_1, G_2) \\ &= \Pr(\boldsymbol{\theta}_{i,1} \in A^s, \boldsymbol{\theta}_{i',2} \in A^s|A^s \neq \emptyset, G_1, G_2)\Pr(A^s \neq \emptyset) + \\ & \Pr(\boldsymbol{\theta}_{i,1} \in A^s, \boldsymbol{\theta}_{i',2} \in A^s|A^s = \emptyset, G_1, G_2)\Pr(A^s = \emptyset) \end{aligned}$$

$$= \Pr(\boldsymbol{\theta}_{i,1} \in A^s, \boldsymbol{\theta}_{i',2} \in A^s | A^s \neq \emptyset, G_1, G_2) \Pr(A^s \neq \emptyset)$$

Then $\Pr(A^s \neq \emptyset) = 1 - \Pr(A^s = \emptyset) = 1 - \prod_{k=1}^{\infty} \{p_1(1-p_2) + p_2(1-p_1)\} = 1$. This is since at each atom k , G_j selects the atom with probability p_j and $G_{j'}$ does not select the atom, with probability $(1-p_{j'})$, or vice versa. Denote $K^s = \{k : \phi_k \in A^s\}$ and $K^j = \{k : \phi_k \in A^j\}$. The term $\Pr(\boldsymbol{\theta}_{i,1} \in A^s, \boldsymbol{\theta}_{i',2} \in A^s | A^s \neq \emptyset, G_1, G_2)$ is evaluated as

$$\Pr(\boldsymbol{\theta}_{i,1} \in A^s, \boldsymbol{\theta}_{i',2} \in A^s | A^s \neq \emptyset, G_1, G_2) = \left[\sum_{k \in K^s} \pi_{1,k} \right] \left[\sum_{k \in K^s} \pi_{2,k} \right].$$

Since $\Pr(A^s \neq \emptyset) = 1$, $|K^s| \geq 1$. And since $\pi_{1,k} > 0$ and $\pi_{2,k} > 0$ for $k \in K^s$, for some arbitrary $k^* \in K^s$, we have

$$\Pr(\boldsymbol{\theta}_{i,1} \in A^s, \boldsymbol{\theta}_{i',2} \in A^s | A^s \neq \emptyset, G_1, G_2) \geq \pi_{1,k^*} \pi_{2,k^*} > 0$$

Therefore,

$$\Pr(\boldsymbol{\theta}_{i,1} \in A^s, \boldsymbol{\theta}_{i',2} \in A^s | G_1, G_2) = \Pr(\boldsymbol{\theta}_{i,1} \in A^s, \boldsymbol{\theta}_{i',2} \in A^s | A^s \neq \emptyset, G_1, G_2) \times 1 > 0.$$

And the first term in (A.13) is

$$\begin{aligned} \Pr(\boldsymbol{\theta}_{i,1} = \boldsymbol{\theta}_{i',2} | \boldsymbol{\theta}_{i,1} \in A^s, \boldsymbol{\theta}_{i',2} \in A^s) &= \mathbb{E}[\Pr(\boldsymbol{\theta}_{i,1} = \boldsymbol{\theta}_{i',2} | G_1, G_2, \boldsymbol{\theta}_{i,1} \in A^s, \boldsymbol{\theta}_{i',2} \in A^s)] \\ &= \mathbb{E} \left[\left(\sum_{\phi_k \in A^s} I(\boldsymbol{\theta}_{i,1} = \boldsymbol{\theta}_{i',2} = \phi_k) p(\phi_k) \right) | G_1, G_2, \boldsymbol{\theta}_{i,1} \in A^s, \boldsymbol{\theta}_{i',2} \in A^s \right] \\ &= \mathbb{E} \left[\left(\sum_{\phi_k \in A^s} \pi_{1,k} \pi_{2,k} p(\phi_k) \right) | G_1, G_2, \boldsymbol{\theta}_{i,1} \in A^s, \boldsymbol{\theta}_{i',2} \in A^s \right] \end{aligned}$$

$$\begin{aligned}
& \stackrel{(a)}{=} \sum_{k \in K^s} \mathbb{E}[\pi_{1,k}] \mathbb{E}[\pi_{2,k}] = \sum_{k \in K^s} \mathbb{E} \left\{ \pi'_{1,k} \prod_{l \in K^1, l < k} (1 - \pi'_{1,l}) \right\} \mathbb{E} \left\{ \pi'_{2,k} \prod_{l \in K^2, l < k} (1 - \pi'_{2,l}) \right\} \\
& \geq \sum_{k \in K^s} \mathbb{E} \left\{ \pi'_{1,k} \prod_{l \in K^1, l < k} (1 - \pi'_{1,l}) \prod_{l \in K^{1^c}, l < k} (1 - \pi'^*_{1,l}) \right\} \mathbb{E} \left\{ \pi'_{2,k} \prod_{l \in K^2, l < k} (1 - \pi'_{2,l}) \prod_{l \in K^{2^c}, l < k} (1 - \pi'^*_{2,l}) \right\} \\
& \stackrel{(b)}{=} \sum_{k \in K^s} [\mathbb{E}[\beta_k]^2] \stackrel{(c)}{=} \sum_{k \in K^s} \left[\frac{1}{1 + \gamma} \left(\frac{\gamma}{1 + \gamma} \right)^{k-1} \right]^2
\end{aligned}$$

where $\pi'^*_{j,l} \sim \text{Beta}(\alpha_0 \beta_k, \alpha_0 (1 - \sum_{l=1}^k \beta_l))$, and K^{j^c} s are the complement sets of K^j $j = 1, 2$. In addition, (a) is true because

$$p(\phi_k | G_j) = \begin{cases} 1 & \text{if } \phi_k \in G_j \\ 0 & \text{o.w.} \end{cases},$$

and (b) is true because the term $\pi'_{j,k} \prod_{l \in K^j, l < k} (1 - \pi'_{j,l}) \prod_{l \in K^{j^c}, l < k} (1 - \pi'^*_{j,l}) = \pi'^*_{j,k} \prod_{l < k} (1 - \pi'^*_{j,l})$ for $k \in K^s$ (i.e., equation (1)), with conditional expectation (condition on β) equal to β_k , and (c) is true because $\beta_k = \beta'_k \prod_{l < k} (1 - \beta'_l)$, $\beta'_k \sim \text{Beta}(1, \gamma)$.

Again since $|K^s| \geq 1$, for some arbitrary $k^* \in K^s$, we have

$$\sum_{k \in K^s} \left[\frac{1}{1 + \gamma} \left(\frac{\gamma}{1 + \gamma} \right)^{k-1} \right]^2 \geq \left[\frac{1}{1 + \gamma} \left(\frac{\gamma}{1 + \gamma} \right)^{k^*-1} \right]^2 > 0.$$

Thus, we have

$$\Pr(\theta_{i,1} = \theta_{i',2} | \theta_{i,1} \in A^s, \theta_{i',2} \in A^s) > 0.$$

Combine with $\Pr(\theta_{i,1} \in A^s, \theta_{i',2} \in A^s | A^s \neq \emptyset, G_1, G_2) > 0$, we have now shown that

$$\Pr(\theta_{i,1} = \theta_{i',2} | G_1, G_2) > 0,$$

which completes the proof. \square

A.9 Proof of Theorem 4

We derive the mean of G_j . Recall $G_0 = \sum_{k=1}^{\infty} \beta_k \delta_{\phi_k}$. Then conditional on G_0 is equivalent to conditional on $\beta' = \{\beta'_k\}_{k=1}^{\infty}$ and $\Phi = \{\phi_k\}_{k=1}^{\infty}$. From equation (A.11) in the proof of proposition 1, we have

$$\mathbb{E}[G_j|G_0] = \mathbb{E}[G_j|\beta', \Phi] = \sum_{k=1}^{\infty} \mathbb{E}[\pi_{j,k}|\beta'] \delta_{\phi_k} = \sum_{k=1}^{\infty} \bar{p} \beta'_k \prod_{l < k} (1 - \bar{p} \beta'_l) \delta_{\phi_k}.$$

Recognizing that $\beta'_k \sim \text{Beta}(1, \gamma)$ and $\phi_k \sim H$, we have $\mathbb{E}[G_j|G_0] = G^*$, where $G^* \sim \text{FSBP}(\bar{p}, \gamma, H)$, by definition of FSBP in Section 2. \square

A.10 Additional Details on Posterior Inference

More details on the slice-efficient sampler To sample β'_k conditional on the other parameters and data, we use an Metropolis-Hastings (MH) step to sample from

$$p(\beta'_k | \dots) \propto \prod_{\{(j,l) | \forall j, l \geq k, \pi'_{j,l} \neq 0\}} p_{\text{Beta}} \left(\pi'_{j,l} | \alpha_0 \beta_l, \alpha_0 \left(1 - \sum_{s=1}^l \beta_s \right) \right) \times p(\beta'_k) \quad (\text{A.14})$$

where $p_{\text{Beta}}(\cdot | a, b)$ is the p.d.f of beta distribution, $\beta_k = \beta'_k \prod_{l=1}^{k-1} (1 - \beta'_l)$, and $p(\beta'_k) = p_{\text{Beta}}(\cdot | 1, \gamma)$. In addition, we use a uniform distribution as the proposal density function: $\beta'_{k_{\text{prop}}} \sim \text{Unif}(\beta'_{k_{\text{curr}}} - \epsilon, \beta'_{k_{\text{curr}}} + \epsilon)$, where $\beta'_{k_{\text{prop}}}$ is the proposal, $\beta'_{k_{\text{curr}}}$ is the β'_k in current iteration, and $\epsilon \in (0, 1)$ is the step size. If $\beta'_{k_{\text{prop}}} < 0$, we set $\beta'_{k_{\text{prop}}} = |\beta'_{k_{\text{prop}}}|$, and if $\beta'_{k_{\text{prop}}} > 1$, we set $\beta'_{k_{\text{prop}}} = 2 - \beta'_{k_{\text{prop}}}$. It can be shown the proposal density is symmetric.

To sample p_j , we have

$$p_j | \dots \propto p_j^{\sum_k 1(\pi'_{j,k} \neq 0) + a - 1} (1 - p_j)^{\sum_k 1(\pi'_{j,k} = 0) + b - 1}.$$

Denoting $m_{j,0} = \sum_{k=1}^{K^*} 1(\pi'_{j,k} = 0)$ the number of zero weights, we can sample p_j as

$$p_j | \dots \sim \text{Beta}(a + K^* - m_{j,0}, b + m_{j,0}) \quad (\text{A.15})$$

If we assume that the concentration parameters α_0 and γ are random with gamma priors, we can sample them using the procedure described in Escobar and West [1995] and Teh et al. [2004]. In Teh et al. [2004], the authors show that the full conditional of α_0 and γ is based on a matrix $\mathbf{W} = \{w_{j,k}\}$ that records the number of tables in restaurant j serving dish k according to the Chinese restaurant franchise process, and the posterior of this matrix depends only on \mathbf{Z} and β . We use equation (40) of Teh et al. [2004] to construct a latent matrix \mathbf{W} and then follow the same method as the HDP to sample both concentration

parameters.

Label switching As shown in the manuscript, we use the ECR algorithm of Papastamoulis and Iliopoulos [2010] to resolve the issue of label switching. This algorithm post-processes the MCMC samples using label permutations. The idea behind ECR is based on the invariance of likelihood with respect to the permutation of component labels.

For each MCMC iteration with label matrix $\mathbf{Z}^{(m)} = \{z_{i,j}^{(m)}\}$, $z_{i,j}^{(m)} \in \{1, \dots, K\}$, where the superscript (m) denotes the m th MCMC iteration, we can form a partition of the $N = \sum_{j=1}^J n_j$ observations based on $\mathbf{Z}^{(m)}$. We denote the corresponding unique labels of $\mathbf{Z}^{(m)}$ as $\mathbf{t}^{(m)} = \{t_1^{(m)}, \dots, t_K^{(m)}\}$, $t_k^{(m)} \in \{1, \dots, K\}$. For example, suppose we have a sample of $N = 7$ observations across $J = 2$ groups, $\mathbf{y} = \begin{bmatrix} y_{1,1} & y_{2,1} & y_{3,1} \\ y_{1,2} & y_{2,2} & y_{3,2} & y_{4,2} \end{bmatrix}$, and two iterations of MCMC samples, i.e., $m = 1$ and $m = 2$, both partitioned the observations into the same 3 clusters, i.e., Cluster A = $\{y_{1,1}, y_{1,2}, y_{2,2}\}$, Cluster B = $\{y_{2,1}, y_{3,1}\}$, and Cluster C = $\{y_{3,2}, y_{4,2}\}$, according to their corresponding $\mathbf{Z}^{(1)}$ and $\mathbf{Z}^{(2)}$. However, in each of the two MCMC iterations, different labels of $\mathbf{t}^{(1)} = \{1, 2, 3\}$, with $\mathbf{Z}^{(1)} = \begin{bmatrix} 1 & 2 & 2 \\ 1 & 1 & 3 & 3 \end{bmatrix}$, and $\mathbf{t}^{(2)} = \{2, 1, 3\}$, with $\mathbf{Z}^{(2)} = \begin{bmatrix} 2 & 1 & 1 \\ 2 & 2 & 3 & 3 \end{bmatrix}$ are assigned to the observations. Thus, there is a switched label of Cluster A and Cluster B through $m = 1$ and $m = 2$. To resolve the label-switching issue, the method finds a permutation of labels at each MCMC iteration, denote as $\boldsymbol{\tau}^{(m)}(\mathbf{t}^{(m)})$, such that, compare to a reference label, say $\mathbf{t}^{(1)}$, $\boldsymbol{\tau}^{(2)}(\mathbf{t}^{(2)}) = \mathbf{t}^{(1)} = \{1, 2, 3\}$.

Specifically, the ECR method first picks an MCMC sample from one iteration (e.g., one close to MAP) as the reference label. Then, the method iterates over each MCMC sample of parameters of interest to find a random permutation of labels corresponding to the equivalent allocation of the reference label. We then switch the labels accordingly for all model parameters related to the cluster labels, i.e., label matrix \mathbf{Z} , MCMC samples

of cluster weights $\{\pi_{j,k}\}$, and cluster means $\{\phi_k\}$. The ECR method is implemented in **R** package **label.switching** [Papastamoulis, 2015]. We use ECR to relabel the MCMC samples of the weights. After permuting the weights according to the result of ECR, we then explore the MCMC samples of the permuted weights for all j groups to learn the common and unique clusters in the groups.

A.11 Additional Simulation Data and Results in Section 5.2

Figure A.1 shows the data distribution of the randomly selected sample, with sample size of 150, in scenario one of simulation studies. The $G1$ to $G6$ refers to group 1 to group 6.

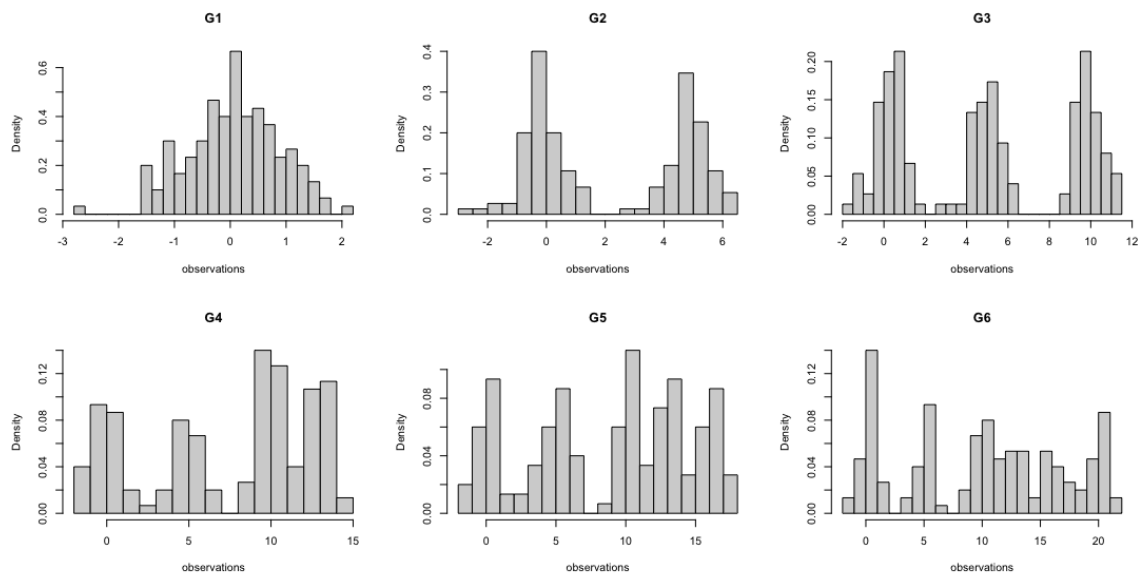


Figure A.1: Data distribution for randomly selected sample with sample size of 150 in scenario one.

Table A.2 shows the mean and cluster weights of simulation setup for the multivariate data in scenario two. Table A.3 shows the number of common clusters across all groups for

scenario one.

Figure A.2 shows the posterior distribution of the number of clusters in each group, the number of common clusters for group 6, and the number of unique clusters for scenario one.

		Cluster 1	Cluster 2	Cluster 3	Cluster 4	Cluster 5
True mean		$\begin{pmatrix} -6 \\ 4 \\ -6 \end{pmatrix}$	$\begin{pmatrix} -3 \\ 2 \\ -3 \end{pmatrix}$	$\begin{pmatrix} 0 \\ 0 \\ 0 \end{pmatrix}$	$\begin{pmatrix} 3 \\ -2 \\ -3 \end{pmatrix}$	$\begin{pmatrix} 6 \\ -4 \\ -6 \end{pmatrix}$
True weights	Group 1	0.2	0.2	0.2	0.2	0.2
	Group 2	0.3	0	0.5	0.2	0
	Group 3	0	0.6	0.4	0	0

Table A.2: Ground truth of cluster means and weights for scenario two in the simulation. Here, cluster 3 is common shared by all three groups.

		Group 1	Group 2	Group 3	Group 4	Group 5	Group 6
Number clusters	CAM	1/1	2/2	3/3	4/4	5/5	6/5
	HDP	1/1	2/2	3/3	4/4	5/5	6/4
	PAM	1/1	2/2	3/3	4/4	5/5	6/5
Unique clusters	CAM	0/0	0/0	0/0	0/0	0/0	1/0
	HDP	0/0	0/0	0/0	0/0	0/0	1/0
	PAM	0/0	0/0	0/0	0/0	0/1	1/1
		G6 vs. G5	G6 vs. G4	G6 vs. G3	G6 vs. G2	G6 vs. G1	All Groups
Common clusters	CAM	5/5	4/4	3/3	2/2	1/1	1/1
	HDP	5/4	4/3	3/3	2/2	1/1	1/1
	PAM	5/4	4/4	3/3	2/2	1/1	1/1

Table A.3: Simulated univariate data. Estimated number of clusters and number of unique clusters in each group, and estimated number of common clusters between groups for the three methods, CAM, HDP, and PAM. Entries x/y represent ground truth/point estimate based on the optimal partition.

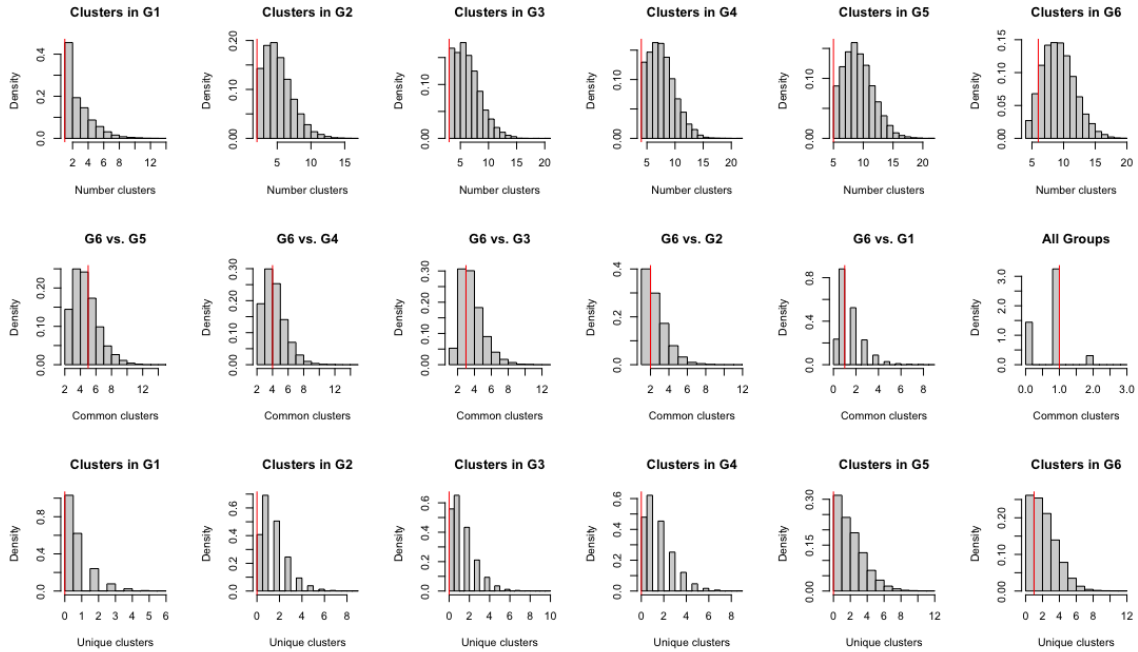


Figure A.2: PAM posterior distributions for (top row) number of clusters in each group, (middle row) number of common clusters in selected groups, and (bottom row) the number of unique clusters in each group. The red vertical lines are the ground truth.

A.12 Additional Distributions and Results of Microbiome Population in Section 6.1

Figure A.3 shows the histogram of OTU counts for the four randomly selected individuals in the analysis of Microbiome dataset.

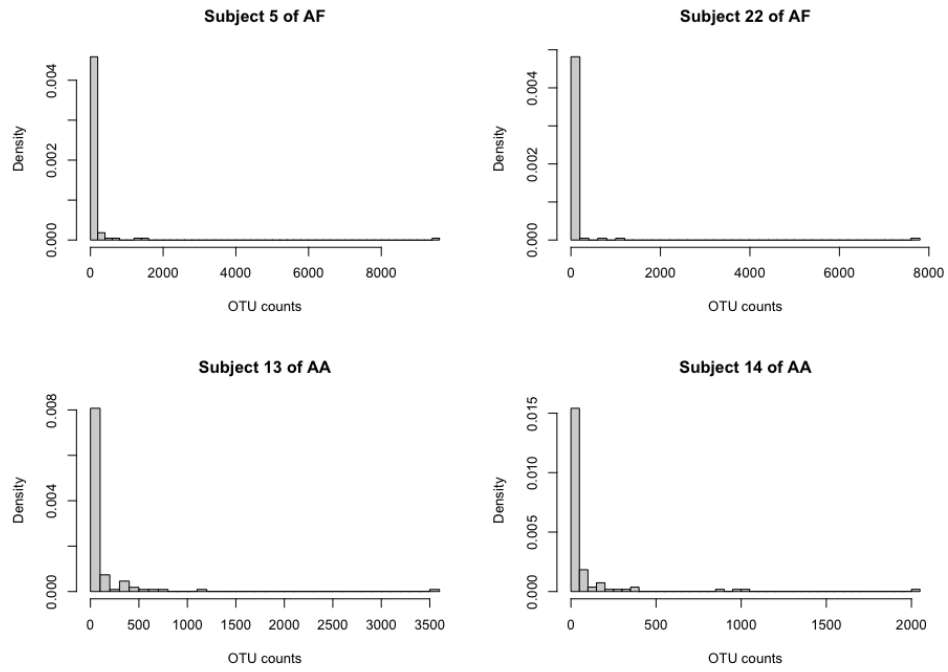


Figure A.3: Histograms of the microbiome population of four selected individuals.

Figure A.4 shows the heatmap of the number of common clusters between each pair of individuals.

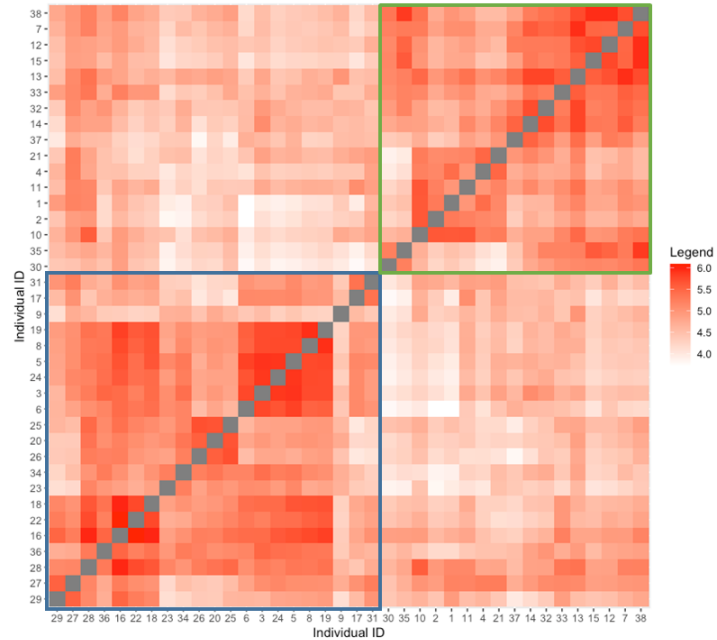


Figure A.4: Heatmap of the number of common clusters between any pair of individuals in the Microbiome study. A dark red color indicates a high number of common clusters and a white color indicates a low number. The cluster in the bottom left (blue box) of the heatmap consists of 13 individuals from AF with eight from AA, while the cluster in the top right (green box) consists of 13 AAs and four AFs.

A.13 Additional Results of Warts Dataset Analysis in Section 6.2

Figure A.5 below shows the cluster membership of each patient of the Warts dataset.

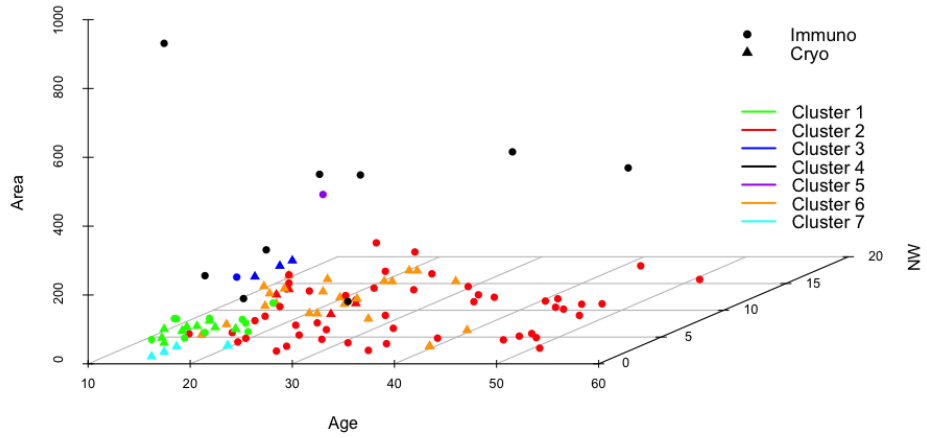


Figure A.5: Estimated cluster membership of patients in the warts dataset based on the optimal partition. The cluster labels are shown with different colors, across two groups indicated by the circles and triangles. The clustering result is based on four covariates, and we plot three of them, area, age, and number of warts (NW).